WILEY

Cooperative path following of constrained autonomous vehicles with model predictive control and event-triggered communications

Nguyen T. Hung[1] | Antonio M. Pascoal[1] | Tor A. Johansen[2]

[1]Institute for Systems and Robotics (ISR), Instituto Superior Técnico (IST), University of Lisbon, Lisbon, Portugal

[2]Center for Autonomous Marine Operations and Systems (AMOS), Norwegian University of Science and Technology (NTNU), Trondheim, Norway

Correspondence
Nguyen T. Hung, Institute for Systems and Robotics (ISR), Instituto Superior Técnico, University of Lisbon, Av. Rovisco Pais 1, 1049-001 Lisbon, Portugal.
Email: hungnguyen@isr.ist.utl.pt

Present address
Nguyen T. Hung, IST, Torre Norte, Piso 8, Av. Rovisco Pais, 1 Lisbon, 1049-001, Portugal.

Funding information
FCT Project UID/EEA/5009/2013; H2020 EU Marine Robotics Research Infrastructure Network, 731103; Marine UAS project under the Marie Curie Sklodowska grant agreement, 642153; Research Council of Norway, 223254

Summary

We present a solution to the problem of multiple vehicle cooperative path following (CPF) that takes explicitly into account vehicle input constraints, the topology of the intervehicle communication network, and time-varying communication delays. The objective is to steer a group of vehicles along given spatial paths, at speeds that may be path dependent, while holding a feasible geometric formation. The solution involves decoupling the original CPF problem into two subproblems: (i) single path following of input-constrained vehicles and (ii) coordination of an input-constrained multiagent system. The first is solved by adopting a sampled-data model predictive control scheme, whereas the latter is tackled using a novel distributed control law with an event-triggered communication (ETC) mechanism. The proposed strategy yields a closed-loop CPF system that is input-to-state-stable with respect to the system's state (consisting of the path following error of all vehicles and their coordination errors) and the system's input, which includes triggering thresholds for ETC communications and communication delays. Furthermore, with the proposed ETC mechanism, the number of communications among the vehicles are significantly reduced. Simulation examples of multiple autonomous vehicles executing CPF maneuvers in 2D under different communication scenarios illustrate the efficacy of the CPF strategy proposed.

KEYWORDS
consensus, cooperative path following, event-triggered communications, MPC, multiagent system

1 | INTRODUCTION

Cooperative path following, an important class of multiple vehicle formation control, is defined as the problem of steering a group of vehicles along a set of spatial paths, at speeds that may be path dependent, while holding a feasible geometric pattern. Among a myriad of applications related to cooperative path following (CPF), we single out those involving unmanned aerial vehicles (UAVs) for coastal monitoring,[1,2] and autonomous marine vehicles (AMVs) for marine habitat

---

Abbreviations: AMV, autonomous marine vehicle; CPF, cooperative path following; ETC, event-triggered communication; ISS, input-to-state-stable; MPC, model predictive control; UAVs, unmanned aerial vehicles.

TABLE 1 CPF categories

Categories		Literature
Vehicle inputs	Unconstrained	2,4,5,9,12
	Constrained	7,8
Communications	Continuous	2,4,14-16
	Periodic	5
	Event-based	9,10,12
Speed profile	Constant	2,12
	Path dependent	2,4,10

mapping and geotechnical surveying.[3] From a control design and analysis standpoint, CPF may be viewed as exhibiting a two-layer control structure: the lower layer, called *path following*, in charge of making a group of vehicles converge to a set of desired paths parametrized in an appropriately normalized manner, while the upper layer, referred to as networked multiagent system (MAS) coordination layer, has the goal of synchronizing the path parameters and making them evolve at the same normalized desired speed profile along the paths. Under these circumstances, proper path parametrization will ensure that the vehicles will reach a desired formation with the assigned individual speed profiles compatible with the paths and the formation (see References 4 and 5 for an introduction to these concepts). Using this setup, different approaches to the CPF problem have been proposed in the literature. A simple categorization of the methods used is presented in Table 1.

Most approaches assume that the vehicles' inputs (eg, speed and heading rate) are unconstrained. This assumption allows designers to use a wide range of classical nonlinear control methods such as Lyapunov-based techniques to design controllers for *path following*, while the *coordination* problem is tackled by resorting to tools from network control theory for *unconstrained* MAS, see for example, Reference 6 for a comprehensive introduction to consensus algorithms and its applications in cooperative control. However, in practice the inputs of the vehicles are always saturated at certain levels due to intrinsically physical limitations. As a consequence, controllers designed for unconstrained vehicles may fail to yield adequate performance. Even worse, stability of the resulting closed loop systems may be seriously compromised if the vehicle constraints are not taken directly into account during the design process.

Due to its ability to handle explicitly input constraints, model predictive control (MPC) has recently been proposed as a key enabling tool for the solution of CPF problems, see for example References 7 and 8. In Reference 7, the authors propose an MPC scheme to solve the path following problem, while the coordination problem is solved using a classical consensus law. However, the approach in Reference 7 has two limitations. First, the MPC scheme is designed based on a linearization of the path following error system, which implies that stability of the resulting system is only guaranteed locally. In addition, with the consensus law used in Reference 7 there is no guarantee that the total speed assigned to each vehicle, which is the summation of the nominal desired speed and the correction speed issued by the consensus law satisfy the vehicle's speed constraint. In Reference 8, the authors address the CPF problem using a distributed MPC framework. However, the methodology adopted requires that the speed of vehicles be allowed to be negative, a constraint that is practically impossible to meet for some classes of autonomous vehicles such as fixed-wing UAVs or AMVs.

Another factor that plays a key role in the design of CPF control systems stems from the limitations naturally imposed by the requirement that the agents exchange data over a given communication network. From a purely theoretical standpoint, it is common in the literature to assume that communications occur continuously in time. In this situation, each vehicle has permanent access to the information provided by its neighbors to include it in some form of consensus law. In practice, however this assumption is clearly violated, namely in applications where communication networks exhibit low bandwidth and nonnegligible transmission latency. To cope with this situation, it is crucial to explicitly incorporate in the design process the fact that communications do not take place continuously. A possible solution is to consider periodic communications, with the latter taking place at discrete instants of time only.[5] Recently, with the objective of further reducing the rate of interagent communications in cooperative MAS control, event-triggered communications have come to the fore. Representative examples include the work in References 9 and 10 on CPF that exploits the concept of logic-based communications advanced in Reference 11 and that in Reference 12 which build upon an event-triggered communication (ETC) mechanism introduced in Reference 13. Temporary communication losses are taken into account in References 4 and 14 but only for the case when communications occur continuously.

An important issue in the design of CPF systems is the parametrization of the paths to be followed and the specification of the desired, identical rate of evolution of the path parameters, which can be viewed as a desired normalized speed profile for the agents involved to track. If the desired speed is constant, the coordination problem can be cast in the form of a linear MAS consensus problem[12] whereas if the speed is parameterized as a general function of the path parameters (ie, path dependent), the resulting coordination problem is equivalent to a consensus problem of nonlinear MAS.[4,10] However, none of methods described in the literature address the problem of coordination of *nonlinear* MAS with *input constraints* that arises naturally in the context of CPF.

Motivated by the above considerations, this article proposes a CPF control strategy that takes explicitly into account realistic constraints on the vehicles' inputs, the topology of the intervehicle communications network, and communication delays. Specifically, the main contributions of this article include the following:

(i) At the *path following* level, we develop an MPC scheme for *path following* that takes into account explicitly the fact that in a large number of applications the vehicle's linear speed is strictly positive. When compared with existing MPC-based methods (see for example References 7 and 8), the proposed MPC scheme has the advantage of avoiding the construction of a terminal set, thus yielding a global region of attraction for single vehicle path following.

(ii) At the *coordination* level, we propose a novel distributed control strategy for the *coordination of nonlinear* MAS where the agents' *input constraints* are explicitly taken into account. We also propose an ETC mechanism that is not only capable of reducing the frequency of communications among vehicles but is also robust with respect to time-varying communication delays, making the scheme attractive for scalable networks with limited communication bandwidth. This result is not only applicable in the context of CPF for multiple autonomous vehicles, but also for many other applications involving the coordination/synchronization/consensus of nonlinear MAS with input constraints.

The article is organized as follows. Section 2 summarizes the basic notation and reviews key results of graph theory for undirected and connected networks. The problem of interest is formulated formally in Section 3. Section 4 describes the strategy proposed for CPF. Illustrative simulations are presented in Section 5, while Section 6 contains the main conclusions. Finally, the proofs of the main results are given in the Appendices.

2 | PRELIMINARIES

2.1 | Notation

The symbols $\|\cdot\|$ and $\|\cdot\|_\infty$ denote the Euclidean norm and the infinity norm of a vector, respectively. By $\min(\cdot)$ and $\max(\cdot)$, we mean the minimum and maximum values, respectively of a scalar function defined over the real line, whereas $\min\{\cdot\}$ and $\max\{\cdot\}$ denote min and max operators of a finite set of real numbers. Given a map $z : x \rightarrow z(x)$, $z'(x), z''(x)$ represent the first-order and the second-order partial derivative of z with respect to x, respectively. Given a vector $\mathbf{x} = [x_1, x_2, \ldots, x_n]^T \in \mathbb{R}^n$, $\mathbf{tanh}(\mathbf{x}) \in \mathbb{R}^n$ is the vector of tan hyperbolic functions defined by $\mathbf{tanh}(\mathbf{x}) := [\tanh(x_1), \tanh(x_2), .., \tanh(x_n)]^T$. Given a finite set S, $|S|$ is the cardinality of S, that is, the number of elements of S.

2.2 | Graph theory

Let $\mathcal{G}(\mathcal{V}, \mathcal{E})$ (abbv. $\mathcal{G}$) be an undirected graph induced by an intervehicle communication network, where $\mathcal{V}$ denotes the set of the vertices or nodes (each corresponds to a vehicle) and $\mathcal{E}$ is the set of edges (each standing for a data link). $\mathcal{G}$ is said to be connected if there exists a path connecting every two nodes in the graph. Let $\mathcal{N}^{[i]}$ be the set of neighboring nodes of node i with which this node communicates. The adjacency matrix of the graph, denoted A, is a square matrix with rows and columns indexed by the nodes such that the i, j entry of A is 1 if $j \in \mathcal{N}^{[i]}$ and zero otherwise. The degree matrix D of a the graph is a diagonal matrix where the i, i-entry equals $|\mathcal{N}^{[i]}|$, the cardinality of $\mathcal{N}^{[i]}$. The Laplacian matrix of an undirected graph is defined as $L := D - A$. It is well known that if $\mathcal{G}$ is undirected, then L is symmetric and $L\mathbf{1} = \mathbf{0}$, where $\mathbf{1} := [1]_{N \times 1}$ and $\mathbf{0} := [0]_{N \times 1}$ with N is the total number of nodes. Further, if $\mathcal{G}$ is connected, then L has a simple eigenvalue at zero with an associated eigenvector $\mathbf{1}$ and the remaining eigenvalues are all positive. We refer to Reference 6 for a comprehensive introduction to graph theory and its applications to the consensus problems.

3 | PROBLEM FORMULATION

For simplicity of exposition we consider motions in 2D. In what follows, $\{\mathcal{I}\} = \{x_I, y_I\}$ denotes an inertial frame and $\{\mathcal{B}\}^{[i]} = \{x_B^{[i]}, y_B^{[i]}\}$ denotes a body frame attached to vehicle i. We consider a set of $N \geq 2$ vehicles and the corresponding set of N spatial paths that they are required to follow, described by

$$\{\mathcal{P}^{[i]} : \gamma^{[i]} \to [\mathbf{p}_d^{[i]}(\gamma^{[i]}); \psi_d^{[i]}(\gamma^{[i]})] \in \mathbb{R}^3; i \in \mathcal{N}\}, \tag{1}$$

where $\mathcal{N} := \{1, \ldots, N\}$ denotes the set of vehicles, $\gamma^{[i]}$ is the variable parameterizing path i, $\mathbf{p}_d^{[i]}(\gamma^{[i]}) = [x_d^{[i]}(\gamma^{[i]}), y_d^{[i]}(\gamma^{[i]})]^T; i \in \mathcal{N}$ is the position vector of a generic point on the path i expressed in the inertial frame, and $\psi_d^{[i]}(\gamma^{[i]}); i \in \mathcal{N}$ is the angle that the tangent to path i at point $\mathbf{p}_d^{[i]}(\gamma^{[i]})$ makes with x_I. Let $\mathbf{p}^{[i]} = [x^{[i]}, y^{[i]}]^T; i \in \mathcal{N}$ be the position vector of the center of mass of vehicle i expressed in the inertial frame. Assuming that the vehicles have negligible sway speed, their kinematic models are given by

$$\dot{x}^{[i]} = u^{[i]} \cos \psi^{[i]}, \dot{y}^{[i]} = u^{[i]} \sin \psi^{[i]}, \dot{\psi}^{[i]} = r^{[i]}, \tag{2}$$

where $u^{[i]}, \psi^{[i]}, r^{[i]}; i \in \mathcal{N}$ denote the speed, yaw angle, and yaw rate of vehicle i, respectively. Due to physical limitations of the vehicles, we consider that the speed and the heading rate are constrained, that is, $(u^{[i]}, r^{[i]}) \in \mathbb{U}^{[i]}$, for all $i \in \mathcal{N}$, where $U^{[i]}$ is referred as an input constraint set for vehicle i, defined explicitly as

$$\mathbb{U}^{[i]} := \{(u^{[i]}, r^{[i]}) : u_{min}^{[i]} \leq u^{[i]} \leq u_{max}^{[i]}, |r^{[i]}| \leq r_{max}^{[i]}\}. \tag{3}$$

Here, $u_{min}^{[i]} > 0$ and $u_{max}^{[i]}$ are lower and upper bounds on the speed, respectively, and $r_{max}^{[i]}$ is an upper bound on the heading rate. We note that the kinematics model (2) is adequate for a large class of vehicles that include mobile robots,[17] fixed-wing UAVs undergoing planar motion,[7] and a wide class of under-actuated AMVs such as Medusa and Delfim[18]or Charlie,[19] for which the sway speed is in practice so small that it can be neglected. A similar kinematic model with a drift term can be found in Reference 20 for the case where the motion is disturbed by constant wind (for UAVs) or constant ocean current (for AMVs). In addition, it is important to remark that in the present work we require the speeds of the vehicles to be nonnegative. This is due to the fact that for many autonomous vehicles such as marine robots and fixed-wing UAVs, it is very difficult or even impossible to control the vehicle moving backwards. This strict constraint makes the CPF problem more challenging when compared to the case where this type of constraint is not taken into account, as in Reference 8.

In CPF, vehicle i is assigned path i to follow, see the illustration in Figure 1. We consider a scenario where the fleet of vehicles are not only required to follow their assigned paths but also to converge to and maintain a desired geometric formation, while maneuvering with desired speed profiles along the paths compatible with the formation. To solve the constrained CPF problem, the methodology used in this article decouples the constrained CPF problem into two subproblems: *path following of constrained vehicles* to steer the vehicles to converge to their assigned paths and *coordination of constrained MAS* that requires the vehicles to exchange information regarding their progression along the paths (as measured by their path parameters) and negotiate their speeds to reach the desired formation. Using this setup, we show that
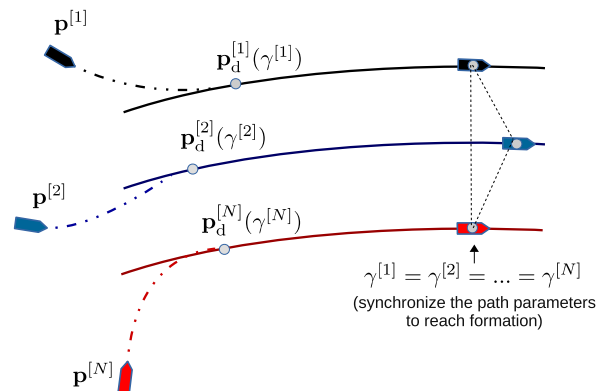
FIGURE 1 Illustration of cooperative path following [Colour figure can be viewed at wileyonlinelibrary.com]

in order to control a fleet of vehicles with a desired formation, the vehicles need to exchange very limited information; in this case, a simple scalar path-related parameter that is used for coordination. From a communication and practical implementation perspective, this is an advantageous feature of the proposed CPF when compared with other formation approaches such as distributed MPC that normally requires more information to be exchanged among the vehicles, see for example References 21 and 22.

3.1 | Single path following of constrained vehicles

In this subsection, we formulate the problem of *single vehicle constrained path following* to make a vehicle converge to a path, while ensuring that the speed of the corresponding path parameter tracks a desired speed profile. To this end, we exploit the concept of "tracking a virtual reference" introduced in Reference 17. Because in this section we deal with a single vehicle, for the sake of simplicity we drop the superscript [i] in the variables in Equations (1) to (3). Later, in subsequent sections, we will reintroduce the original notation when necessary.

Consider the path following problem for a single vehicle with the kinematics model given by (2), subject to the constraints on the inputs given by (3), following a path parameterized by the variable γ given by (1). Consider a parallel transport frame $\{\mathcal{F}\} = \{x_{\mathcal{F}}, y_{\mathcal{F}}\}$ with its origin at an arbitrary point S on the path and its axes defined as follows: $x_{\mathcal{F}}$ is aligned with the tangent to the path and points in the direction of increasing path length and $y_{\mathcal{F}}$ is determined by rotating $x_{\mathcal{F}}$ 90° clockwise (see Figure 2). In the setup adopted for path-following, the parallel transport frame moves along the path in a manner to be determined and plays the role of a "virtual reference" for the position and heading angle that the vehicle must track to achieve good path following. Let $\mathbf{e}_{\{\mathcal{I}\}} = \mathbf{p} - \mathbf{p}_d(\gamma)$ be position error vector expressed in the inertial frame and $e_\psi = \psi - \psi_d(\gamma)$ be the orientation error between the path and the vehicle. We define $R_{\mathcal{I}}^{\mathcal{F}} : \psi_d \to R_{\mathcal{I}}^{\mathcal{F}}(\psi_d) :=$ $[\cos(\psi_d), \sin(\psi_d); -\sin(\psi_d), \cos(\psi_d)]$ as the rotation matrix from the inertial frame to the parallel transport frame. Let $\mathbf{e}_{\{\mathcal{F}\}} = [e_x, e_y]^T$ be the position error expressed in the parallel transport frame, computed as $\mathbf{e}_{\{\mathcal{F}\}} = R_{\mathcal{I}}^{\mathcal{F}} \mathbf{e}_{\{\mathcal{I}\}}$. Collectively, defining $\mathbf{x} = [e_x, e_y, e_\psi]^T \in \mathbb{R}^3$ as the path following error vector and using the methodology exposed in[17] for wheeled robots, the evolution of the path following error in the parallel transport frame is described by the dynamic equations

$$\dot{\mathbf{x}} = \mathbf{f}(\mathbf{x}, \mathbf{u}) = \begin{bmatrix} -g(\gamma)v(1 - \kappa(\gamma)e_y) + u\cos(e_\psi) \\ -\kappa(\gamma)g(\gamma)ve_x + u\sin(e_\psi) \\ r - \kappa(\gamma)g(\gamma)v \end{bmatrix}, \tag{4}$$

where $g(\gamma) := \sqrt{(x_d'(\gamma))^2 + (y_d'(\gamma))^2}$, $\kappa(\gamma) = \left(x_d'(\gamma)y_d''(\gamma) - x_d''(\gamma)y_d'(\gamma)\right)/g^3(\gamma)$, and $v = \dot{\gamma}$ is the speed of the path parameter that gives an extra degree of freedom in the process of designing path following controllers; $\kappa(\gamma)$, by definition, is the curvature along the path and $\mathbf{u} := [u, v, r]^T$ is the input vector of the path following error system.

Notice that we have introduced a new input v to control the evolution of the path parameter γ. Later, for the purpose of designing an input constrained path following controller, v should lie in a constraint set $\mathbb{U}_v$, defined explicitly as

$$\mathbb{U}_v := \{v : |v| \le v_{\max}\}, \tag{5}$$

where $v_{\max}$ is a design parameter that will be specified.

We are now in a position to formulate the following constrained path following problem.
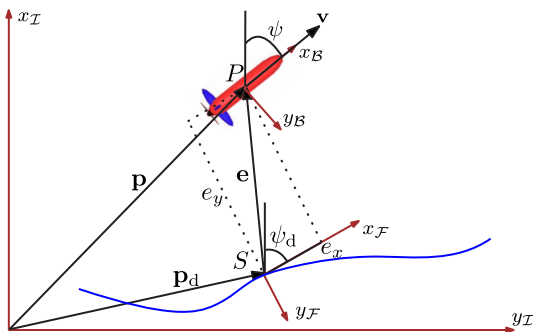
FIGURE 2 Vehicle and reference frames. Velocity vector in the body frame $\mathbf{v} = [u, 0]$. P is the center of mass of the vehicle and S is the origin of the parallel transport frame at a point on the path [Colour figure can be viewed at wileyonlinelibrary.com]

Problem 1. [Constrained Path Following] Given a spatial path $\mathcal{P}$ parameterized by γ, a desired positive and bounded speed profile $v_d : \gamma \to v_d(\gamma)$, and the constraint sets for the vehicle's inputs and the speed of the "virtual reference" given by (3) and (5), respectively, derive a feedback control law for $(u, r) \in \mathbb{U}$ and $v \in \mathbb{U}_v$ to fulfill the following tasks:

- Geometric task: drive the path following error $\mathbf{x}$ with the dynamics described in (4) to zero as $t \to \infty$.
- Dynamic task: ensure also that v tracks the desired speed profile $v_d(\gamma)$, that is, $v(t) - v_d(\gamma(t)) \to 0$ as $t \to \infty$.

Stated intuitively, a solution to the input-constrained path following problem consists of adjusting the speed v of the "virtual reference", the speed u, and the heading rate r of the vehicle, subject to given vehicle constraints, to drive the vehicle to the path and keep its velocity vector aligned with the tangent to the path while having the path parameter track the desired speed profile.

Remark 1. If γ is the arc length of the path, then $g(\gamma) \equiv 1$. In this case, the path following error system (4) resembles the path following error system developed in Reference 17. Notice that although parameterizing a path by its arc-length is convenient, the main problem is that it is not always possible to find a closed form expression of the curvature as the function of the arc-length; elliptical and sinusoid paths are examples. In our setup, the path parameter γ in (4) is not necessarily the arc length, thus making the formulation applicable to any path.

Remark 2. Since the path parameter γ is not necessarily the arc-length, in general v is not the speed of the "virtual reference" in the inertial frame. In fact, the latter equals $g(\gamma)v$. Obviously, if γ is the arc-length of the path, then $g(\gamma) \equiv 1$ and v is truly the speed of the "virtual reference" in the inertial frame.

3.2 | Cooperative path following

Before proceeding to the formulation of the multiple vehicle coordination problem, we made the following assumptions.

Assumption 1.

A1.1 Each vehicle is equipped with a path following controller (to be designed later using an MPC scheme) that solves **Problem** 1, where the desired speed profile $v_d(\cdot)$ along the paths is identical for all vehicles.

A1.2 The intervehicle network topology is time invariant.

In what follows, we assume that the paths that the vehicles must follow are appropriately parameterized to ensure that a given formation is reached when the path parameters, also called coordination states, are equal. For example, to make a number of vehicles follow an equal number of concentric circumferences and be aligned radially along their radii, it suffices to parametrize these paths in terms of their normalized lengths, that is, $\gamma^{[i]} = s^{[i]}/2\pi$, where $s^{[i]}$ is the curvilinear abscissa along path i. Clearly, the vehicles are coordinated and maneuver with a desired normalized path dependent speed $v_d(\cdot)$ if $\gamma^{[i]}(t) = \gamma^{[j]}(t)$ and $\dot{\gamma}^{[i]}(t) = \dot{\gamma}^{[j]}(t) = v_d(\gamma^{[i]})$ for all $i, j \in \mathcal{N}$. See Reference 4 for an introduction to these concepts.

The underlying idea to achieve the coordination is described as follows. Assume for the time being that the vehicles maneuver independently and do not attempt to coordinate their motions. Assume that the path following controller makes the vehicle converge to the path asymptotically ($\mathbf{x}^{[i]} = \mathbf{0}$) and ensures also that the path parameter evolves with the desired speed profile ($v^{[i]} = v_d(\gamma^{[i]})$). Asymptotically, in this situation we have

$$\dot{\gamma}^{[i]} = v^{[i]} = v_d(\gamma^{[i]}); \qquad i \in \mathcal{N}. \tag{6}$$

Replacing $v^{[i]} = v_d(\gamma^{[i]})$ and $\mathbf{x}^{[i]} = \mathbf{0}$ in (4), and noticing that $\mathbf{x}^{[i]} = \mathbf{0}$ is the equilibrium point of the path following system (4), the nominal speeds of the vehicles are given by

$$u^{[i]} = g^{[i]}(\gamma^{[i]})v_d(\gamma^{[i]}); \qquad i \in \mathcal{N}. \tag{7}$$

Recall that the desired formation is only achieved when the path parameters reach consensus (or synchronized), that is, $\gamma^{[i]} = \gamma^{[j]}$ for all $i, j \in \mathcal{N}$. This can be accomplished by adjusting the linear speeds of vehicles about the nominal speeds in (7) so as to make all vehicles reach agreement in the coordination states (the path parameters) and maneuver with the

common normalized desired speed $v_d(\cdot)$. Let $g^{[i]}(\gamma^{[i]})v_c^{[i]}$ be the a correction term for the speed of vehicle i, where $v_c^{[i]}$ is a new input aimed at achieving coordination, to be explained later. The resulting speeds for the vehicles are given by

$$u^{[i]} = g^{[i]}(\gamma^{[i]})(v_d(\gamma^{[i]}) + v_c^{[i]}); \qquad i \in \mathcal{N}. \tag{8}$$

Consequently, the dynamics of the path parameters in (6) are now extended as

$$\dot{\gamma}^{[i]} = v_d(\gamma^{[i]}) + v_c^{[i]}; \qquad i \in \mathcal{N}. \tag{9}$$

At this stage, it is clear that the coordination problem is reduced to finding $v_c^{[i]}; i \in \mathcal{N}$ such that the total speed of each vehicle in (8) still satisfies (3), that is,

$$u_{min}^{[i]} \leq g^{[i]}(\gamma^{[i]})(v_d(\gamma^{[i]}) + v_c^{[i]}) \leq u_{max}^{[i]}; \quad i \in \mathcal{N}, \tag{10}$$

and the path parameters are synchronized and evolve with the common speed profile $v_d(\cdot)$. To solve this consensus problem, each vehicle needs to exchange the path parameters (coordination states) with other vehicles. In this work, we consider that each vehicle is capable of communicating bidirectionally with a set of neighboring vehicles. Let $\mathcal{G}$ be the bidirectional (undirected) graph induced by the interconnection network of the vehicles and $\mathcal{N}^{[i]}$ the set of neighboring vehicles of vehicle i. At the coordination layer, we consider each vehicle to be an agent whose dynamics are given by (9). We are now in a position to formulate the coordination problem as follows.

Problem 2. [Coordination of input-constrained MAS] Given a MAS with the dynamics of each agent given by (9) and the network topology of the MAS modeled by the graph $\mathcal{G}$ satisfying Assumption 1, derive a distributed control law for the input $v_c^{[i]}(\gamma^{[i]}, \gamma^{[j]}); j \in \mathcal{N}^{[i]}$, subject to the input constraint (10), such that $(\gamma^{[i]}(t) = \gamma^{[j]}(t)); \forall i, j \in \mathcal{N}$ and $(\dot{\gamma}^{[i]}(t) = v_d(\gamma^{[i]}(t))); \forall i \in \mathcal{N}$ as $t \to \infty$.

Note that since the function $v_d(\cdot)$ is common for all agents, reaching consensus in the path parameters and their speeds implies that $v_c^{[i]}$ converges to zero for all $i \in \mathcal{N}$. In next section, the process of designing controllers to solve the problems defined above shall be illustrated.

4 | CONTROLLER DESIGN AND MAIN RESULTS

Based on the idea of decoupling the constrained CPF problem into the subproblem of *path following* and *MAS coordination*, we propose a distributed CPF control system that, for each vehicle, exhibits the architecture depicted in Figure 3. The objective of the coordination block is to compute the correction speed $v_c^{[i]}$. An ETC mechanism is proposed to reduce communications among vehicles so that they will only communicate with its neighbors when found necessary, according to some specific criterion. Once the correction speed has been computed, the MPC controller is used to make the vehicle converge to and follow its assigned path. In other words, the MPC controller is used to stabilize the path following error between the vehicle and its assigned path. To make the constrained CPF problem solvable, we assume that given the vehicles' input constraints, the planed paths given in (1) and the desired speed profile $v_d(\cdot)$ are smooth and satisfy the following conditions.

Condition 1.

C1.1 $v_d(\cdot)$ is bounded, that is, $0 < v_{dmin} \leq v_d(\cdot) \leq v_{dmax}$.
C1.2 Condition on the linear speeds:
    There exists a constant $c_u > 0$ such that $u_{min}^{[i]} + c_u \leq g^{[i]}(\gamma^{[i]})v_d(\gamma^{[i]}) \leq u_{max}^{[i]} - c_u$ for all $\gamma^{[i]}$ and $i \in \mathcal{N}$.
C1.3 Condition on the turning rates:
    There exists a constant c_r such that $|\kappa^{[i]}(\gamma^{[i]})g^{[i]}(\gamma^{[i]})v_d(\gamma^{[i]})| < r_{max}^{[i]} - c_r$ for all $\gamma^{[i]}$ and $i \in \mathcal{N}$.

Remark 3. The above conditions are necessary to ensure that the CPF problem is solvable. To see this, notice in C1.2 that the term $g^{[i]}(\gamma^{[i]})v_d(\gamma^{[i]})$ is the nominal desired linear speed, computed in the inertial frame, that vehicle i must track, see (7). Therefore, c_u gives room for the vehicles to adjust their linear speeds about the nominal ones in order to achieve

FIGURE 3 CPF control system for vehicle ith with the ETC mechanism [Colour figure can be viewed at wileyonlinelibrary.com]

coordination, see (8). Similarly, in C1.3, the left hand side of the inequality is the nominal desired heading rate of vehicle i. Hence, c_r gives room for the vehicles to adjust their heading rates about the nominal ones in order to converge to and follow their assigned paths.

Example 1. For paths consisting of straight lines and segments of circumferences, such as lawn mowing paths, the above conditions can be significantly simplified. For example, for straight-line paths, if the paths are parameterized by their arc-lengths, then $g^{[i]}(\gamma^{[i]}) \equiv 1$ for all $i \in \mathcal{N}$. Hence, condition C1.3 can be relaxed and C1.2 is equivalent with $u_{\min}^{[i]} + c_u \leq v_d(\gamma^{[i]}) \leq u_{\max}^{[i]} - c_u$ for all $i \in \mathcal{N}$. In this case c_u can be simply specified as $c_u = \min\{v_{dmin} - u_{\min}^{[i]}, u_{\max}^{[i]} - v_{dmax}\}$ for all $i \in \mathcal{N}$.

In the following subsection, we shall propose distributed control laws with different communication scenarios to update the correction speed $v_c^{[i]}, i \in \mathcal{N}$.

4.1 | Distributed controllers with an ETC mechanism for the coordination problem

Before introducing distributed control laws to solve the coordination problem (**Problem** 2), we define new variables given by

$$z^{[i]} := \int_0^{\gamma^{[i]}} \frac{1}{v_d(\gamma)} d\gamma, \quad i \in \mathcal{N}. \tag{11}$$

Intuitively, $z^{[i]}$ measures the amount of time taken by agent i to travel from 0 to the state $\gamma^{[i]}$. With the above definition, and since $v_d(\gamma) > 0$ for all γ, it follows that the path parameters $\gamma^{[i]}; i \in \mathcal{N}$ are synchronized (or reach consensus), that is, $\gamma^{[i]} = \gamma^{[j]}$ for all $i, j \in \mathcal{N}$ iff the variables $z^{[i]}; i \in \mathcal{N}$ are synchronized, that is, $z^{[i]} = z^{[j]}$ for all $i, j \in \mathcal{N}$. For the sake of convenience, let $\mathbf{z} = [z^{[1]}, z^{[2]}, \ldots, z^{[N]}]^T \in \mathbb{R}^N$ and $\bar{z} = \frac{1}{N} \sum_{i=1}^N z^{[i]}$ be the average of $\mathbf{z}$. We define the coordination error vector

$$\xi = \mathbf{z} - \bar{z}\mathbf{1} = W\mathbf{z}, \tag{12}$$

where $W = I_N - \mathbf{1}\mathbf{1}^T/N$. Clearly, if the variables $z^{[i]}; i \in N$ reach consensus, then $\mathbf{z}$ spans $\mathbf{1}$. Further, since $W\mathbf{1} = \mathbf{0}$, the variables $z^{[i]}; i \in \mathcal{N}$ reach consensus iff $\xi = \mathbf{0}$. Thus, the problem of driving the variables $z^{[i]}; i \in \mathcal{N}$ to reach consensus amounts to driving the coordination error vector ξ to the origin. For this reason, in what follows we propose distributed control laws for $v_c^{[i]}$ for all $i \in \mathcal{N}$ under different communication scenarios to drive the error vector ξ to zero.

Remark 4. Notice that the matrix W is similar to the projection matrix Π_ξ defied in Reference 2, which is popularly used for analyzing consensus of multi agent systems on undirected graphs. The variable $z^{[i]}$ defined in (11) generalizes the coordination state ξ_i given in Reference 2, where the paths are parameterized by their arc-lengths.

4.1.1 | Continuous communications

For clarity of presentation of the concepts involved, we start by assuming that communications take place instantaneously.

Theorem 1 (Coordination with continuous communications). *Consider* **Problem** 2. *Let Condition* 1 *hold for all* $i \in \mathcal{N}$ *and let* $\mathcal{G}$ *be an undirected and connected graph. Then, the distributed control law for* $v_c^{[i]}$; $i \in \mathcal{N}$ *given by*

$$v_c^{[i]} = -k_c^{[i]} \tanh(\sum_{j \in \mathcal{N}^{[i]}} z^{[i]} - z^{[j]}); \ i \in \mathcal{N}, \tag{13}$$

where $z^{[i]}$ *is given by (11) and* $k_c^{[i]}$ *are positive gains satisfying the conditions*

$$0 < k_c^{[i]} \leq c_u / g_{max}^{[i]}; \quad i \in \mathcal{N},$$
$$g_{max}^{[i]} = \max(g^{[i]}(\gamma^{[i]})) \tag{14}$$

drives all the agents' states (path parameters) to reach consensus asymptotically. In other words, the origin of the coordination error vector ξ *is globally asymptotically stable.*

Proof. See Appendix C.1. ∎

The next corollary applies to the special case where the desired speed profile $v_d(\cdot)$ is constant.

Corollary 1. *Consider* **Problem** 2 *and let the conditions stated in Theorem* 1 *hold. Further assume that the speed profile is constant, that is,* $v_d(\gamma^{[i]}) \equiv c > 0$ *for all* $i \in \mathcal{N}$. *Then, the distributed control law for* $v_c^{[i]}$; $i \in \mathcal{N}$ *given by*

$$v_c^{[i]} = -k_c^{[i]} \tanh(\sum_{j \in \mathcal{N}^{[i]}} \gamma^{[i]} - \gamma^{[j]}); \ i \in \mathcal{N}, \tag{15}$$

where $k_c^{[i]}$ *satisfies (14) drives all the agents' states (path parameters) to reach consensus asymptotically.*

It is interesting to observe that in the case of a constant speed profile, the distributed control law does not depend on the desired speed profiles $v_d(\cdot)$. Further, it follows from (15) that the computation of $v_c^{[i]}$ is simplified because there is no need for a block of integrators to compute $z^{[i]}$.

4.1.2 | ETC mechanism without communication delays

The distributed control law proposed in Section 4.1.1 relies on continuous communications among the vehicles. However, this assumption is impossible to meet because practical communication systems require the exchange of data to take place at discrete instants of time. Motivated by this observation, we propose an ETC mechanism in which the vehicles only need to exchange data with their neighbors when necessary, in accordance with an appropriately defined criterion.

In the ETC mechanism, instead of using the true neighboring states ($\gamma^{[j]}$; $j \in \mathcal{N}^{[i]}$), the control law (13) uses their estimates. The underlying idea is that if any agent can produce "good" estimates of the neighboring states, then there is no need to communicate continuously among the vehicles. Let $\hat{\gamma}^{[ij]}$ be an estimate of $\gamma^{[j]}$ computed by agent i (the procedure to compute this estimate will be explained later). The event-triggered distributed control law that we propose is given by

$$v_c^{[i]} = -k_c^{[i]} \tanh\left(\sum_{j \in \mathcal{N}^{[i]}} (z^{[i]} - \hat{z}^{[ij]})\right); i \in \mathcal{N}, \tag{16}$$

where

$$\hat{z}^{[ij]} := \int_0^{\hat{\gamma}^{[ij]}} \frac{1}{v_d(\gamma)} d\gamma, \tag{17}$$

and $k_c^{[i]}$ satisfies condition (14) for all $i \in \mathcal{N}$.

The control law in (16) can be rewritten as

$$v_{\mathrm{c}}^{[i]} = -k_{\mathrm{c}}^{[i]} \tanh\left(\sum_{j \in \mathcal{N}^{[i]}} (z^{[i]} - z^{[j]} + e^{[j]})\right); i \in \mathcal{N}, \tag{18}$$

where,

$$e^{[j]} = z^{[j]} - \hat{z}^{[ij]} = \int_{\hat{\gamma}^{[ij]}}^{\gamma^{[j]}} \frac{1}{v_{\mathrm{d}}(\gamma)} \mathrm{d}\gamma; j \in \mathcal{N}^{[i]}, i \in \mathcal{N}. \tag{19}$$

Notice that $v_{\mathrm{d}}(\gamma)$ is bounded below by v_{dmin}, hence

$$|e^{[j]}(t)| \leq |\gamma^{[j]}(t) - \hat{\gamma}^{[ij]}(t)|/v_{\mathrm{dmin}}; j \in \mathcal{N}^{[i]}, i \in \mathcal{N}. \tag{20}$$

It can be seen that compared with the control law for continuous communications in (13), $v_{\mathrm{c}}^{[i]}$ in (18) has the contribution of the estimation error $e^{[j]}$. The underlying idea in the proposed ETC mechanism is that if $e^{[j]}; j \in \mathcal{N}^{[i]}, i \in \mathcal{N}$ can be enforced to be bounded then, as we will show later, the coordination error ξ will also be bounded. To bound $e^{[j]}$, we define for every agent the variable $\hat{\gamma}^{[j]}; j \in \mathcal{N}$ as a "replica" of $\hat{\gamma}^{[ij]}; i \in \mathcal{N}^{[j]}$. Thus, if we can enforce the estimation error $\tilde{\gamma}^{[j]} := \gamma^{[j]} - \hat{\gamma}^{[j]} = \gamma^{[j]} - \hat{\gamma}^{[ij]}$ to be bounded, then from (20) $e^{[j]}$ will be bounded for all $j \in \mathcal{N}$.

We now introduce a mechanism to synchronize $\hat{\gamma}^{[i]}$ and $\hat{\gamma}^{[ij]}$ for all $i \in \mathcal{N}$ and $j \in \mathcal{N}^{[i]}$ (note that because the graph is symmetric, this is similar to synchronize $\hat{\gamma}^{[j]}$ and $\hat{\gamma}^{[ij]}$ for all $j \in \mathcal{N}$ and $i \in \mathcal{N}^{[j]}$). Let $\{t_k^{[i]}\}; k \in \mathbb{N}$ be the sequence of time instants at which vehicle i sends its current value of $\gamma^{[i]}(t_k^{[i]}); k \in \mathbb{N}$ to its neighbors $j; j \in \mathcal{N}^{[i]}$. During the interval $\mathcal{T}_k^{[i]} := [t_k^{[i]}, t_{k+1}^{[i]})$ we propose the following estimator for $\hat{\gamma}^{[i]}$. For $t \in \mathcal{T}_k^{[i]}$:

$$\dot{\hat{\gamma}}^{[i]}(t) = v_{\mathrm{d}}(\hat{\gamma}^{[i]}(t)), \tag{21a}$$

$$\hat{\gamma}^{[i]}(t_k^{[i]}) = \gamma^{[i]}(t_k^{[i]}); i \in \mathcal{N}. \tag{21b}$$

Equation (21b) implies that whenever agent i broadcasts $\gamma^{[i]}$ to its neighbors, the initial condition for $\hat{\gamma}^{[i]}$ will be reset. Similarly, let $\{t_k^{[ji]}\}; k \in \mathbb{N}$ be the sequence of time instants at which agent $j; j \in \mathcal{N}^{[i]}$ receives the state of agent i. The estimator for $\hat{\gamma}^{[ji]}; j \in \mathcal{N}^{[i]}, i \in \mathcal{N}$ in the interval $\mathcal{T}_k^{[ji]} := [t_k^{[ji]}, t_{k+1}^{[ji]})$ is proposed as follows:

For $t \in \mathcal{T}_k^{[ji]}$:

$$\dot{\hat{\gamma}}^{[ji]}(t) = v_{\mathrm{d}}(\hat{\gamma}^{[ji]}(t)), \tag{22a}$$

$$\hat{\gamma}^{[ji]}(t_k^{[ji]}) = \gamma^{[i]}(t_k^{[i]}); j \in \mathcal{N}^{[i]}, i \in \mathcal{N}. \tag{22b}$$

Equation (22b) implies that whenever agent j receives the state of agent i, the initial condition for $\hat{\gamma}^{[ji]}$ will be reset.

Remark 5. The dynamics of the estimators for $\hat{\gamma}^{[i]}$ and $\hat{\gamma}^{[ji]}$, given by (21a) and (22a), respectively, are motivated by the observation that once coordination is achieved, $\gamma^{[i]} = \gamma^{[j]}$ for all $i, j \in \mathcal{N}$, $v_{\mathrm{c}}^{[i]}$ tends to zero for all $i \in \mathcal{N}$, and all path parameters evolve with the same speed profile $v_{\mathrm{d}}(\cdot)$. As a consequence, in this specific situation the estimators truly represent the dynamics of the path parameters. See Figure 4 for an illustration of the synchronization between $\hat{\gamma}^{[i]}$ and $\hat{\gamma}^{[ji]}$ for all $i \in \mathcal{N}$ and $j \in \mathcal{N}^{[i]}$.

To ensure that the estimation error $\tilde{\gamma}^{[i]}; i \in \mathcal{N}$ bounded, we allow agent i to transmit $\gamma^{[i]}$ whenever $\tilde{\gamma}^{[i]}$ hits a designed bounded threshold that, in general, can be parameterized by a function of time that we call $\eta^{[i]}(t)$. Formally, we define an event-triggering function $h^{[i]}(t)$ for the communication as
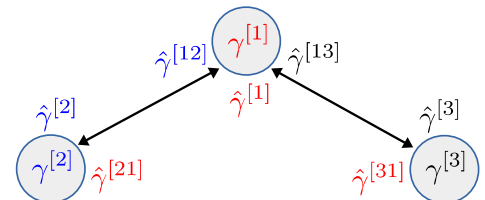
FIGURE 4 The ETC mechanism for the case of negligible delays; $\hat{\gamma}^{[i]}$ and $\hat{\gamma}^{[ji]}$ are synchronized, that is, $\hat{\gamma}^{[i]}(t) = \hat{\gamma}^{[ji]}(t)$ for all t and $j \in \mathcal{N}^{[i]}, i \in \mathcal{N}$ [Colour figure can be viewed at wileyonlinelibrary.com]

$$h^{[i]}(t) = |\tilde{\gamma}^{[i]}(t)| - \eta^{[i]}(t), \tag{23}$$

where $\eta^{[i]}(t)$ belongs to a class of nonnegative functions $\mathcal{C}$ defined by $\mathcal{C} := \{f : R_{\geq 0} \to R_{\geq 0} | 0 \leq f(t) \leq \bar{c}\}$ for all $i \in \mathcal{N}$, where $\bar{c}$ is a uniform upper bound for the function. For example, $\eta^{[i]}(t) = c_1 + c_2 e^{-\alpha t}$ with a proper choice of c_1, c_2 and α is a typical function belonging to $\mathcal{C}$. With the above definition, agent $i; i \in \mathcal{N}$ will send its state to its neighbors whenever $h^{[i]}(t) \geq 0$.

In summary, with the proposed ETC mechanism the following results hold.

Lemma 1. *Suppose there are no communication delays. In this case, the ETC mechanism will ensure that for all t and* $i \in \mathcal{N}, j \in \mathcal{N}^{[i]}$

i) $\hat{\gamma}^{[i]}(t) = \hat{\gamma}^{[ji]}(t)$ *and*
ii) $|\tilde{\gamma}^{[i]}(t)| = |\gamma^{[i]}(t) - \hat{\gamma}^{[i]}(t)| = |\gamma^{[i]}(t) - \hat{\gamma}^{[ji]}(t)| \leq \eta^{[i]}(t).$

Proof. See Appendix A.1 ∎

We show next that with the ETC mechanism proposed above, and in the absence of communication delays, the coordination system satisfies an adequate input-to-state-stable (ISS) condition.

Theorem 2 (Coordination with ETC and without delays). *Consider* **Problem** 2 *and let the conditions stated in Theorem* 1 *hold. Further, let the coordination system be driven by the proposed ETC mechanism and the distributed control law given in* (16). *Then, the closed-loop coordination error system is (ISS) with respect to the state* ξ *and the input* $\eta := [\eta^{[1]}, \ldots, \eta^{[N]}]^{\mathrm{T}}$.

Proof. See Appendix C.2. ∎

Remark 6. Due to space limitations, we refer the reader to definition 4.7 in Reference 23 for the concept of ISS systems. In plain terms, the result in Theorem 2 implies that: (i) if the input η is bounded then the state ξ is bounded and (ii) if $\eta(t) \to \mathbf{0}$ as $t \to \infty$ then $\xi(t) \to \mathbf{0}$ as $t \to \infty$, see the convergent input-convergent state property of an ISS system in Reference 24.

Remark 7. The above ETC mechanism extends the event-triggered mechanism for single integrator MAS described in Reference 25. It also generalizes the triggering condition in Reference 26, where the threshold functions $\eta^{[i]}$ are constant for all $i \in \mathcal{N}$. Compared to Reference 26, this gives more flexibility to reduce the frequency of communications among the vehicles by customizing the triggering threshold function $\eta^{[i]}(t); i \in \mathcal{N}$.

Remark 8. Another concern with any event-triggered control or communication mechanism is that if it can guarantee Zeno-free behavior. With the proposed ETC mechanism in this article, provided that the lower bound on the threshold function $\eta^{[i]}$ is positive for all $i \in \mathcal{N}$ then it can be shown that the minimum-interevent time for every agents is strictly positive; which implies that Zeno behavior can be excluded. Intuitively, this implies that if the lower bound of $\eta^{[i]}$ is positive then it always takes a period of time for the estimation error $|\tilde{\gamma}^{[i]}|$ to reach the triggering threshold $\eta^{[i]}$, which is the condition to generate a new event for communication. The proof of this property is lengthy and involved. However, the proof can be done in a similar to that in Theorem 1 of Reference 27.

Clearly, Theorem 1 is a special case of Theorem 2 when $\eta^{[i]}(t) \equiv 0$ for all $i \in \mathcal{N}$. That is, $\eta^{[i]}(t) \equiv 0$ implies that the triggering condition (23) is satisfied at all times, making the vehicles communicate continuously. To reduce the frequency of communications, the threshold functions $\eta^{[i]}$ can be designed such that they are not necessarily identically equal to zero but $\eta^{[i]}(t) \to 0$ as $t \to \infty; i \in \mathcal{N}$. Then, due to the ISS property, the coordination error ξ will converge to zero as $t \to \infty$. In this setup, the triggering threshold $\eta^{[i]}$ plays the role of a tuning knob to trade off performance of coordination against the cost of communications.

4.1.3 | ETC mechanism with communication delays

In this subsection, we consider more realistic scenarios where the communication delays are time varying and nonhomogeneous. To handle communication delays, we modify slightly the proposed ETC mechanism as follows:

Consider a generic agent i with neighbors $j; j \in \mathcal{N}^{[i]}$. We recall that $t_k^{[i]}$ is the time at which agent i broadcasts its state $(\gamma^{[i]}(t_k^{[i]}))$ to its neighbors and $t_k^{[ji]}$ is the time at which agent j receives that information. Notice that without delay, agent j would receive $\gamma^{[i]}(t_k^{[i]})$ immediately, that is, $t_k^{[ji]} = t_k^{[i]}$. We now consider the case when agent j can only receive the

message broadcast by agent i after a certain time delay denoted $\Delta_k^{[ji]}$. This delay is not known in advance but we assume it can be estimated by agent j. For example, if all agents are equipped with synchronized clocks and, instead of sending only the coordination state $\gamma^{[i]}(t_k^{[i]})$, agent i also sends the tagged time $t_k^{[i]}$, then the time delay can be easily computed as $\Delta_k^{[ji]} = t_k^{[ji]} - t_k^{[i]}$. In general, we define the time delay signal as a function of time, as follows:

$$\Delta_k^{[ji]}(t) = \begin{cases} t - t_k^{[i]}, \text{if } t_k^{[i]} \le t \le t_k^{[ji]}, \\ 0, \text{otherwise}. \end{cases} \tag{24}$$

Notice how with this definition $\Delta_k^{[ji]}(t_k^{[ji]}) = t_k^{[ji]} - t_k^{[i]}$. We now modify the ETC mechanism proposed in previous section to make it robust against communication delays. To this end, the estimator (22) is modified as follows.

For $t \in \mathcal{T}_k^{[ji]}$,

$$\dot{\hat{\gamma}}^{[ji]}(t) = v_\mathrm{d}(\hat{\gamma}^{[ji]}(t)), \tag{25a}$$

$$\hat{\gamma}^{[ji]}(t_k^{[ji]}) = \gamma^{[i]}(t_k^{[i]}) + \int_{t_k^{[i]}}^{t_k^{[ji]}} v_\mathrm{d}(\hat{\gamma}^{[ji]}(\tau))\mathrm{d}\tau. \tag{25b}$$

These equations show that when agent $j; j \in \mathcal{N}^{[i]}$ receives $\gamma^{[i]}(t_k^{[i]})$ from agent i, $\hat{\gamma}^{[ji]}$ is reset to the initial value given by (25b). Compared to (22b), the last term in (25b) acts as a "compensation" term for the estimate of $\hat{\gamma}^{[ji]}$ in order to deal with the time delay $\Delta_k^{[ji]}$.

To see how the modified ETC mechanism is robust against delays, similarly to the case without delays we examine the estimation error $\gamma^{[i]} - \hat{\gamma}^{[ji]}$, which, as we will see later, contributes to the degradation in performance of the coordination error system. To this end, we define $\overline{\eta}^{[i]}(t) := \sup_{\tau \in [0,t]} \eta^{[i]}(\tau)$ as the upper bound for $\eta^{[i]}(\tau)$ up to time t and $\overline{\Delta}^{[i]}(t) := \sup_{\tau \in [0,t]} \{\Delta_k^{[ji]}(\tau); j \in \mathcal{N}^{[i]}, t_k^{[i]} \in [0,t]\}$ as the upper bound for the time delays associated with the messages sent by agent i up to time t. We obtain the following result for the estimation error.

Lemma 2. *Consider the modified ETC mechanism with time-varying delays. Then, for all $t \ge 0$ and $i \in \mathcal{N}, j \in \mathcal{N}^{[i]}$*

$$|\gamma^{[i]}(t) - \hat{\gamma}^{[ji]}(t)| \le \overline{\eta}^{[i]}(t) + (v_\mathrm{dmax} - v_\mathrm{dmin} + k_\mathrm{max})\overline{\Delta}^{[i]}(t), \tag{26}$$

where $k_\mathrm{max} := \max_{i \in \mathcal{N}} k_\mathrm{c}^{[i]}$.

Proof. See Appendix A.2. ∎

Let $\overline{\eta} = \mathrm{col}(\overline{\eta}^{[i]}) \in \mathbb{R}^N$ and $\overline{\Delta} = \mathrm{col}(\overline{\Delta}^{[i]}) \in \mathbb{R}^N$ and define

$$\sigma = \overline{\eta} + (v_\mathrm{dmax} - v_\mathrm{dmin} + k_\mathrm{max})\overline{\Delta}. \tag{27}$$

We obtain the following result for coordination with communication delays.

Theorem 3 (ETC mechanism and communication delays). *Consider **Problem 2** and let the conditions stated in Theorem 1 hold. Let the coordination system be driven by the modified ETC mechanism with the distributed control law given in (16). Then, the closed-loop coordination error system is ISS with respect to the state ξ and the input σ.*

Proof. See Appendix C.3. ∎

Clearly, the results stated in Theorem 3 generalize the results in Theorems 1 and 2. The result in Theorem 2 is a special case of that of Theorem 3 when the communication delays are zero, that is, $\overline{\Delta}(t) \equiv 0$. In this case, the coordination error system is ISS respect to the input $\overline{\eta}$. Furthermore, if both $\overline{\Delta}(t) \equiv 0$ and $\overline{\eta}(t) \equiv 0$, then $\sigma \equiv 0$. In this case, we recover the result of Theorem 1, that is, $\xi = 0$ is GAS.

Remark 9. It is remarked that having synchronized clocks on the vehicles to compute time delays is not a strong assumption. It is relevant to point out that with current technology it is neither difficult nor overly expensive to have synchronized clocks (with a drift of less than 200 nanoseconds in 24 hours) on-board of all the vehicles that are part of a formation. This solution was recently implemented and tested in the scope of the EU WiMUST project.[28]

4.2 | MPC for constrained path following

Section 4.1 provided a solution to the computation of the correction speed $v_c^{[i]}$ in order to achieve coordination. With the correction speed, the total speeds assigned to the vehicles are given by

$$u^{[i]} = (v_d(\gamma^{[i]}) + v_c^{[i]})g^{[i]}(\gamma^{[i]}); i \in \mathcal{N}. \tag{28}$$

As shown in the proof of Lemma 1, the reference speed for $u^{[i]}$, given by (28), satisfies the constraint $u_{\min}^{[i]} \leq u^{[i]} \leq u_{\max}^{[i]}$ for all $i \in \mathcal{N}$. Replacing the vehicle speed u in (4) by (28) for vehicle i, the resulting path following error system for vehicle i is given by

$$\dot{\mathbf{x}}^{[i]} = \mathbf{f}^{[i]}(\mathbf{x}^{[i]}, \mathbf{u}^{[i]}) = \begin{bmatrix} g^{[i]}(\gamma^{[i]}) \left(-v^{[i]}(1 - \kappa^{[i]}(\gamma^{[i]})e_y^{[i]}) + (v_d(\gamma^{[i]}) + v_c^{[i]})\cos(e_\psi^{[i]}) \right) \\ g^{[i]}(\gamma^{[i]}) \left(-\kappa^{[i]}(\gamma^{[i]})v^{[i]}e_x^{[i]} + (v_d^{[i]} + v_c^{[i]})\sin(e_\psi^{[i]}) \right) \\ r^{[i]} - \kappa^{[i]}(\gamma^{[i]})g^{[i]}(\gamma^{[i]})v^{[i]} \end{bmatrix}, \tag{29}$$

where $\mathbf{u}^{[i]} = (v^{[i]}, r^{[i]})$. It follows from (3) and (5) that $\mathbf{u}^{[i]}$ is constrained to the set

$$\mathbb{U}_{pf}^{[i]} := \{(v^{[i]}, r^{[i]}) : |v^{[i]}| \leq v_{\max}^{[i]} \text{ and } |r^{[i]}| \leq r_{\max}^{[i]}\}. \tag{30}$$

We are now in a position to design an MPC scheme to drive the path following error system (29) to zero subject to the input constraint set $\mathbb{U}_{pf}^{[i]}$ defined by (30).

We define a finite horizon open loop optimal control problem $\mathcal{OCP}(t, \mathbf{x}^{[i]}(t), \gamma^{[i]}(t), v_c^{[i]}(t), T_p)$ that the sampled-data MPC must solve at every sampling time as follows:

Definition 1. $\mathcal{OCP}(t, \mathbf{x}^{[i]}(t), \gamma^{[i]}(t), v_c^{[i]}(t), T_p)$

$$\min_{\overline{\mathbf{u}}^{[i]}(\cdot)} J^{[i]}\left(\mathbf{x}^{[i]}(t), \gamma^{[i]}(t), v_c^{[i]}(t), \overline{\mathbf{u}}^{[i]}(\cdot)\right),$$

with

$$J^{[i]}(\cdot) := \int_t^{t+T_p} l^{[i]}\left(\overline{\mathbf{x}}^{[i]}(\tau), \gamma^{[i]}(\tau), v_c^{[i]}(\tau), \overline{\mathbf{u}}^{[i]}(\tau)\right) d\tau$$

subject to

$$\dot{\overline{\mathbf{x}}}^{[i]}(\tau) = \mathbf{f}^{[i]}\left(\overline{\mathbf{x}}^{[i]}(\tau), \overline{\mathbf{u}}^{[i]}(\tau)\right), \quad \tau \in [t, t + \mathcal{T}_p], \tag{31a}$$

$$\overline{\mathbf{x}}^{[i]}(t) = \mathbf{x}^{[i]}(t), \tag{31b}$$

$$\overline{v}_c^{[i]}(\tau) = -k_c^{[i]} \tanh\left(\sum_{j \in \mathcal{N}^{[i]}} \overline{z}^{[i]}(\tau) - \overline{\overline{z}}^{[ij]}(\tau)\right), \tag{31c}$$

$$\dot{\overline{\gamma}}^{[i]}(\tau) = v^{[i]}(\tau), \tau \in [t, t + T_p], \overline{\gamma}^{[i]}(t) = \gamma^{[i]}(t), \tag{31d}$$

$$\dot{\overline{\overline{\gamma}}}^{[ij]}(\tau) = v_d(\hat{\gamma}^{[ij]}(\tau)), \tau \in [t, t + T_p], \tag{31e}$$

$$\overline{\overline{\gamma}}^{[ij]}(t) = \hat{\gamma}^{[ij]}(t); \quad j \in \mathcal{N}^{[i]}, \tag{31f}$$

$$\overline{\mathbf{u}}^{[i]}(\tau) \in \mathbb{U}_{pf}^{[i]}, \quad \tau \in [t, t + T_p], \tag{31g}$$

$$\frac{\partial V}{\partial \mathbf{x}^{[i]}} \mathbf{f}^{[i]}(\mathbf{x}^{[i]}(t), \overline{\mathbf{u}}^{[i]}(t)) \leq \frac{\partial V}{\partial \mathbf{x}^{[i]}} \mathbf{f}^{[i]}(\mathbf{x}^{[i]}(t), \mathbf{u}_n(\mathbf{x}^{[i]}(t))). \tag{31h}$$

In the constraint Equations (31), the variables with bar denote predicted variables, to distinguish them from the real variables without a bar. Specifically, $\bar{\mathbf{x}}^{[i]}(\tau)$ is the predicted trajectory of the path following error which is computed using the dynamic model (29) and the initial conditions (31b); $\bar{\gamma}^{[i]}(\tau)$ is the predicted value of the path parameter $\gamma^{[i]}$ driven by the path following input $\bar{\mathbf{u}}^{[i]}(\tau)$; $\bar{\hat{\gamma}}^{[ij]}$ is the prediction of the state of neighboring agent $j; j \in \mathcal{N}^{[i]}$ by using the estimator (25) over the prediction horizon T_{p}; $\bar{z}^{[i]}$ and $\bar{\hat{z}}^{[ij]}$ are computed using (11), (17) with predicted $\bar{\gamma}^{[i]}$ and $\bar{\hat{\gamma}}^{[ij]}$, respectively. The constraint (31h) is referred as a stability constraint to guarantee stability. This constraint is constructed based on a Lyapunov function $V : \mathbb{R}^3 \to \mathbb{R}_{\geq 0}$ and its associated stabilizing constrained control law $\mathbf{u}_{\mathrm{n}} : \mathbb{R}^3 \to \mathbb{U}_{\mathrm{pf}}^{[i]}$. This setup is inspired by the result in[29] to improve the performance of path following. Finally, $l^{[i]} : \mathbb{R}^3 \times \mathbb{R} \times \mathbb{R} \times \mathbb{R}^2 \to \mathbb{R}_{\geq 0}$ is the stage cost of the final horizon cost $J^{[i]}$.

In state feedback sampled-data MPC, the optimal control problem $\mathcal{OCP}(\cdot)$ is repeatedly solved at every discrete sampling instant $t_i = i\delta$, $i \in \mathbb{N}_+$, where δ is a sampling interval. Let $\bar{\mathbf{u}}^{[i]*}(\tau)$ be the optimal solution of the optimal control problem $\mathcal{OCP}(\cdot)$. The MPC control law $\mathbf{u}_{\mathrm{mpc}}^{[i]}(\cdot)$ is then defined as

$$\mathbf{u}_{\mathrm{mpc}}^{[i]}(t) = \bar{\mathbf{u}}^{[i]*}(t) \text{ for } t \in [t_i, t_i + \delta]. \tag{32}$$

Before proceeding to the main result for the path following problem with the proposed MPC scheme, we make the following assumptions.

Assumption 2.

A2.1 The stage cost $l^{[i]}(\cdot)$ is continuous, positive definite, and $l^{[i]}(\cdot) = 0$ when $\bar{\mathbf{x}}^{[i]} = \mathbf{0}$ and $\mathbf{u}_{\mathrm{a}}^{[i]} := [-v^{[i]} + (v_{\mathrm{d}}(\gamma^{[i]}) + v_{\mathrm{c}}^{[i]}) \cos e_{\psi}^{[i]}, r^{[i]} - \kappa^{[i]}(\gamma^{[i]}) g^{[i]}(\gamma^{[i]}) v^{[i]}]^{\mathrm{T}} = \mathbf{0}$.

A2.2 Given the path following error dynamics in (29), there exist a Lyapunov function $V : \mathbb{R}^3 \to \mathbb{R}_{\geq 0}$ such that V is positive definite and $V(\mathbf{x}^{[i]}) = 0$ only for $\mathbf{x}^{[i]} = \mathbf{0}$, and an associated nonlinear feedback control law $\mathbf{u}_{\mathrm{n}} : \mathbb{R}^3 \to \mathbb{U}_{\mathrm{pf}}^{[i]}$ that satisfies $\frac{\partial V}{\partial \mathbf{x}^{[i]}} \mathbf{f}(\mathbf{x}^{[i]}, \mathbf{u}_{\mathrm{n}}(\mathbf{x}^{[i]})) \leq 0$ for all $\mathbf{x}^{[i]}$. Further, $\mathbf{u}_{\mathrm{n}}(\mathbf{x}^{[i]})$ globally stabilizes (29).

We now state an important result for the constrained path following problem using the proposed MPC scheme.

Theorem 4 (Path following with MPC). *Consider the path following error system (29) subject to the input constrained set $\mathbb{U}_{\mathrm{pf}}$ given by (30), controlled by the proposed MPC scheme, and let Assumption 2 hold true. Then, the origin of the path following error is globally asymptotically stable.*

Proof. See Appendix C.4. ∎

The most important requirement in the proposed MPC scheme is the existence of a stabilizing control law $\mathbf{u}_{\mathrm{n}}(\cdot)$ and an associated Lyapunov function $V(\cdot)$ that satisfies Assumption 2. It can be shown that the control law in the following lemma satisfies the assumption.

Lemma 3 (Global Constrained Nonlinear PF Controller). *Consider the path following error system (29) and let $v_{\max}$ in (30) be chosen such that*

$$v_{\mathrm{dmax}} + k_{\mathrm{c}} < v_{\max} < r_{\max}/\max(|\kappa(\gamma) g(\gamma)|). \tag{33}$$

Then, the global Lyapunov-based control law given by

$$\mathbf{u}_{\mathrm{n}}(\mathbf{x}) = \begin{bmatrix} v \\ r \end{bmatrix} = \begin{bmatrix} \frac{1}{g(\gamma)} \left(u \cos(e_{\psi}) + k_1 \tanh(e_x) \right) \\ -\frac{k_3 e_y u \sin(e_{\psi})}{(1 + e_x^2 + e_y^2) e_{\psi}} - k_2 \tanh(e_{\psi}) + \kappa(\gamma) g(\gamma) v \end{bmatrix}, \tag{34}$$

where $k_1, k_2, k_3 \in \mathbb{R}_{>0}$ are tuning parameters that satisfy

$$0 < k_1 \leq v_{\max} \min(g(\gamma)) - (v_{\mathrm{dmax}} + k_c) g_{\max},$$
$$0.5 k_3 u_{\max} + k_2 \leq r_{\max} - \max(|\kappa(\gamma) g(\gamma)|) v_{\max} \tag{35}$$

renders the origin of the path following error system GAS. Further, the Lyapunov function associated with the control law (34), given by

$$V(\mathbf{x}) = \frac{k_3}{2} \ln(1 + e_x^2 + e_y^2) + \frac{1}{2} e_{\psi}^2, \tag{36}$$

satisfies Assumption 2.

Proof. See Appendix A.3. ∎

Remark 10. Notice that for the sake of simplicity we dropped the subscript [*i*] in Equations (33) to (36).

Remark 11. The MPC scheme proposed above is but one possible solution to the problem of stabilizing the path following error system. One can use for example the MPC proposed in Reference 30, where terminal constraints are imposed to guarantee recursive feasibility and stability. However, due to the need of a terminal set, the region of attraction in Reference 30 is local, while the region of attraction for the path following error in Theorem 4 is global. The choice of Lyapunov function in (36) is inspired by the work of tracking mobile robot in Reference 31.

It is obvious that with the constraint (31h) the MPC scheme improves the performance of the closed-loop path following error system compared to the nonlinear control law. A comparative study can be found in References 20 and 26.

5 | OVERALL CLOSED-LOOP CPF SYSTEM

In the previous section, with a view to adopting a decoupling strategy for the design of a CPF system, we proposed a distributed CPF strategy to solve two key problems involved: (i) multiple agent coordination with an ETC mechanism and (ii) MPC for input-constrained path following of each agent. The resulting distributed CPF strategy can be implemented using Algorithm 1 described below. The algorithm embodies in its structure the decoupling methodology adopted, that is, the CPF control system can be seen as a two-layer control structure. In this context, coordination and communications together play the role of an upper layer whose objective is to coordinate the path parameters to reach a desired formation, while the main objective of the path following layer is to steer the vehicles to their assigned paths. In Theorems 3 and 4, we have shown that if the two layers are considered separately, the path following system of each vehicle is GAS while the coordination error that involves the path parameters is ISS respect to the input σ that includes the *trigger threshold* η and the communication delays. In this section, we shall state results for the overall closed-loop CPF system where the interaction of two layers is taken explicitly into account.

Algorithm 1. MPC-CPF with the ETC mechanism for vehicle *i*

1: At every sampled time *t*, vehicle *i* implements following procedures:
2: **procedure** COORDINATION AND COMMUNICATION
3:     **if** $h^{[i]}(t) \geq 0$ **then**
4:         Broadcast $\gamma^{[i]}(t)$;
5:         Reset $\hat{\gamma}^{[i]}$ using (21b);
6:     **end if**
7:     **if** Receive a new message from vehicle *j* **then**
8:         **if** $j \in \mathcal{N}^{[i]}$ **then**
9:             Reset $\hat{\gamma}^{[ij]}$ using (25b);
10:        **end if**
11:    **end if**
12:    Run the estimator (21);
13:    Run the estimator (25);
14:    Update the correction speed $v_c^{[i]}(t)$ using (16);
15: **return** $v_c^{[i]}(t)$
16: **end procedure**
17: **procedure** PATH FOLLOWING
18:     Update the path following error $\mathbf{x}^{[i]}(t)$;
19:     Solve the $\mathcal{OCP}(\cdot)$ problem to find $\bar{\mathbf{u}}^{[i]}(\cdot)$;
20:     Use the MPC control law (32) to update $v^{[i]}(t), r^{[i]}(t)$;
21:     Update the vehicle's speed $u^{[i]}(t)$ using (28);
22: **return** $u^{[i]}(t), r^{[i]}(t), v^{[i]}(t)$
23: **end procedure**

Theorem 5. *Consider the complete closed-loop CPF system composed by*

- *A set of N vehicles, whose motions are described by (2) subject to the input constraints given by (3).*
- *A set of paths given by (1) and the desired speed profiles $v_d(\gamma^{[i]})$ satisfying Condition 1, with all $i \in \mathcal{N}$.*

Let the vehicles be controlled by the proposed MPC-CPF and the ETC mechanism given by Algorithm 1. Then, the overall closed-loop system is ISS respect to the state $\mathbf{x}_{cl} := [\mathbf{x}_{pf}^T, \xi^T]^T$ and the input σ, where $\mathbf{x}_{pf}$ is the state of the path following layer defined as $\mathbf{x}_{pf} := \mathrm{col}(\mathbf{x}^{[i]})$.

Proof. See Appendix C.5. ∎

6 | SIMULATION EXAMPLES

We consider a fleet of five Medusa class of AMVs with the input constraints $u^{[i]} \in [0.2, 2]$meter per second and $r^{[i]} \in [-0.2, 0.2]$radian per second for all $i = \mathcal{N} := \{1, \ldots, 5\}$ (see Reference 3 for the details of the vehicles' specification). The vehicles are required to execute two types of CPF missions as described in Table 2, with the paths parameterized by their normalized arc-lengths. For triangular formations, the vehicles are required to maneuver along parallel paths while adopting the shape of a triangle, see Figure 6, left. For circular formations, the vehicles are required to maneuver along nested circumferences and align themselves radially, see Figure 6, right. In Table 2, for triangular formations, $d^{[i]}$ and $c^{[i]}$ are parameters specifying the desired cross-track and along-track distances between the vehicles, while for circular formations, $a^{[i]}$ are the radii of the circumferences. The communication topology adopted is depicted in Figure 5, which shows the indexes of the vehicles and the bidirectional communication links between them (represented by arrows).

In the proposed MPC scheme, the Lyapunov-based controller in Lemma 3 is used to construct the constraint (31h). The tunning parameters for the Lyapunov-based controller, the coordination controller, and the event-triggering threshold functions are set in Table 3. Notice that the coordination gain $k_c^{[i]}$ is chosen to satisfy conditions (14), while the gains for the Lyapunov-based controller are chosen to satisfy conditions in Lemma 3 for all vehicles. The stage cost for the MPC scheme is defined as the quadratic form

$$l^{[i]}(\cdot) = \bar{\mathbf{x}}^{[i]}(\tau)^T Q \bar{\mathbf{x}}^{[i]}(\tau) + \mathbf{u}_a^{[i]}(\tau)^T R \mathbf{u}_a^{[i]}(\tau),$$

where $Q = \mathrm{diag}(1, 1, 2)$ and $R = \mathrm{diag}(2, 20)$. The sampling interval is set to $\delta = 0.2$ second and the prediction horizon is set to $T_p = 2$ seconds. To solve the finite optimal control problem $\mathcal{OCP}(\cdot)$, we used Casadi, an open source optimization tool described in Reference 32. Communication delays are set $\Delta = 2$ seconds for all transmitted messages and for both missions.

TABLE 2 Planed missions

	Planned paths	v_d
Triangular	$\mathbf{p}_d^{[i]}(\gamma^{[i]}) = [a(\gamma^{[i]} - c^{[i]}), d^{[i]}]^T$, $a = 50\,\mathrm{m}, c^{[1]} = c^{[5]} = 0, c^{[2]} = c^{[4]} = 0.1, c^{[3]} = 0.2$, $d^{[1]} = -10\,\mathrm{m}, d^{[2]} = -5\,\mathrm{m}, d^{[3]} = 0\,\mathrm{m}, d^{[4]} = 5, d^{[5]} = 10\,\mathrm{m}$	0.02
Circular	$\mathbf{p}_d^{[i]}(\gamma^{[i]}) = [a^{[i]} \cos(\gamma^{[i]}), a^{[i]} \sin(\gamma^{[i]})]^T$, $a^{[1]} = 30\,\mathrm{m}, a^{[2]} = 33\,\mathrm{m}, a^{[3]} = 36\,\mathrm{m}$, $a^{[4]} = 39\,\mathrm{m}, a^{[5]} = 42\,\mathrm{m}$	0.02
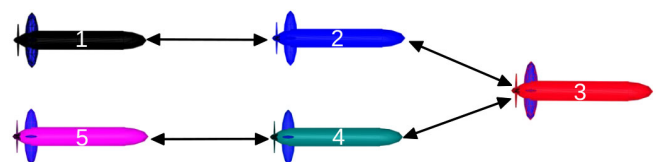
FIGURE 5 Communication topology [Colour figure can be viewed at wileyonlinelibrary.com]

TABLE 3 Controllers setup

Controller	Tuning parameters
Path following	$k_1^{[1]} = 0.3, k_1^{[2]} = 0.33, k_1^{[3]} = 0.36,$
	$k_1^{[4]} = 0.39, k_1^{[5]} = 0.42,$
	$k_2^{[i]} = 0.06, k_3^{[i]} = 0.09, v_{max}^{[i]} = 0.05, \forall i = 1, \dots, 5$
Coordination	$k_c^{[i]} = 0.008, i = 1, \dots, 5$
	$\eta^{[i]}(t) = c_1 e^{-\alpha t} + \epsilon, \forall i = 1, \dots, 5$
	$c_1 = 0.1, \alpha = 0.2, \epsilon = 5\text{e-}3$
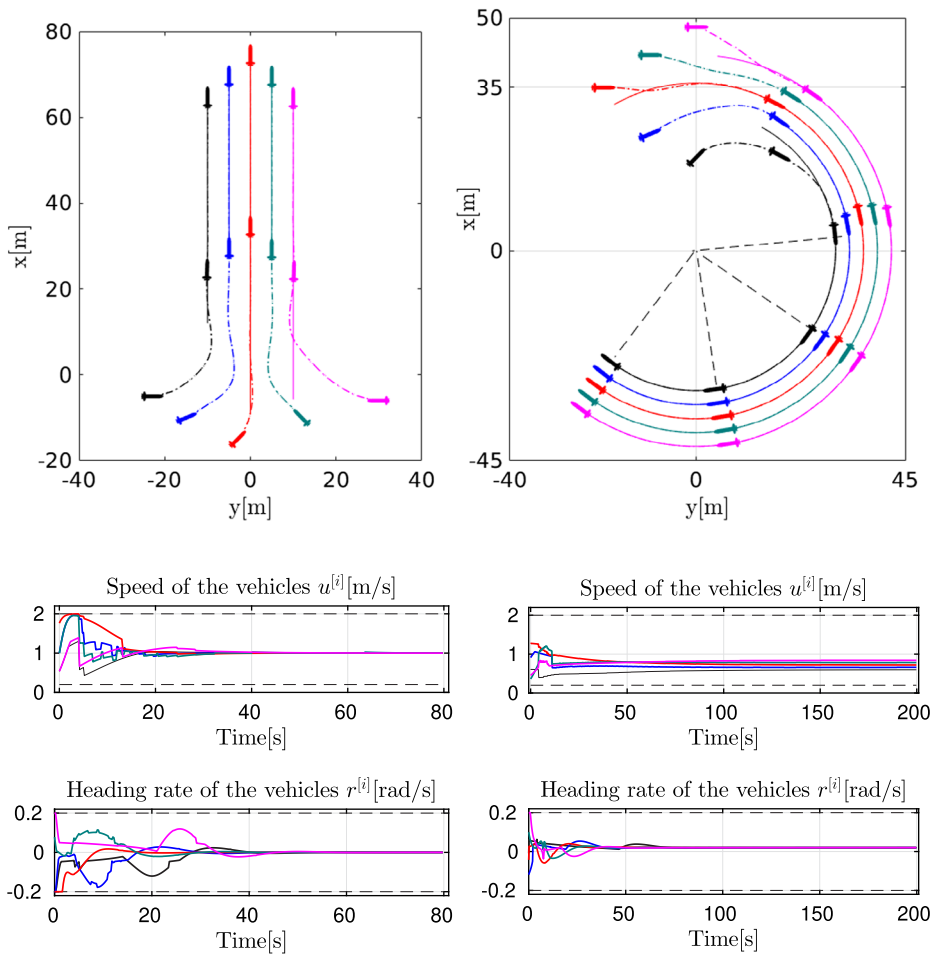
FIGURE 6 Trajectories of the vehicles. Left (triangular formation), right (circular formation). Solid lines are the desired paths, dash-dot lines are the trajectories of the vehicles [Colour figure can be viewed at wileyonlinelibrary.com]

FIGURE 7 Vehicles inputs. Black dash lines are bounds of the inputs [Colour figure can be viewed at wileyonlinelibrary.com]

The trajectories of vehicles are shown in Figure 6. It is visible that the vehicles converge to the desired paths and reach the desired formations in both missions. The performance of the proposed CPF strategy for the two missions is illustrated in Figures 7 to 9. It can be seen from Figure 7 that the inputs of the vehicles produced by the proposed CPF strategy satisfy their constraints. Notice also in Figure 8 how the Lyapunov functions for path following of the vehicles are monotonically decreasing to zero, corroborating the results that the path following errors are asymptotically stable.

Regarding coordination among the vehicles, Figure 9A shows that the coordination states (path parameters) reach consensus asymptotically and evolve with the desired common speed profile v_d. In terms of communications between the vehicles, Figure 9B indicates that at beginning of the simulation, communications take place more frequently. In contrast, when the vehicles reach to the desired formations, they no longer need to communicate. This can be explained with the help of Figure 9C which shows the estimation errors and the triggering threshold functions. At the beginning of the missions, the dynamics of the path parameters are disturbed by the path following system (because the vehicles are away from their paths) and the correction speeds are updated from the coordination system. As a consequence, there are significant errors of the path parameters' estimates. Hence, the estimation errors hit the threshold functions frequently which, in turn, triggers communications more frequently.
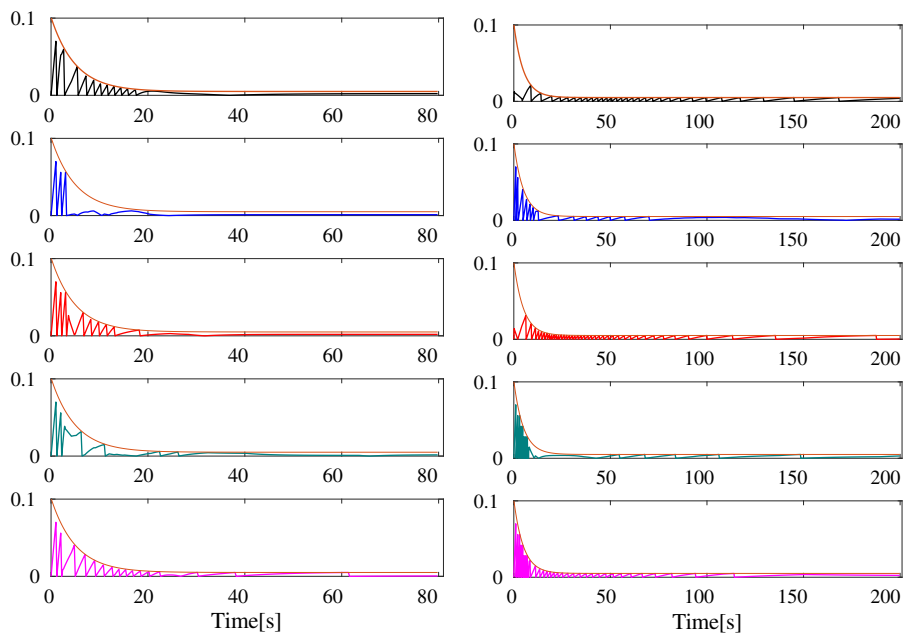
FIGURE 8 Path following
performance: evolution of the Lyapunov
function V for path following [Colour
figure can be viewed at
wileyonlinelibrary.com]
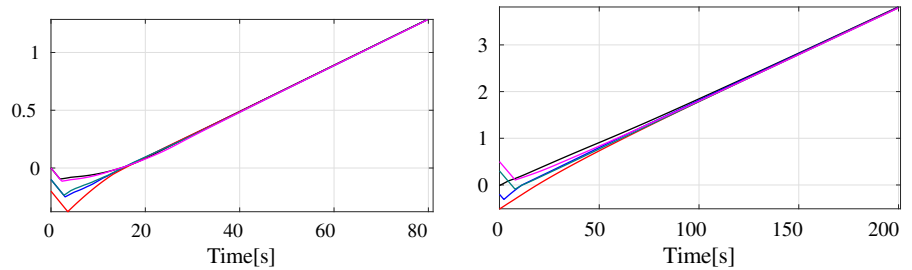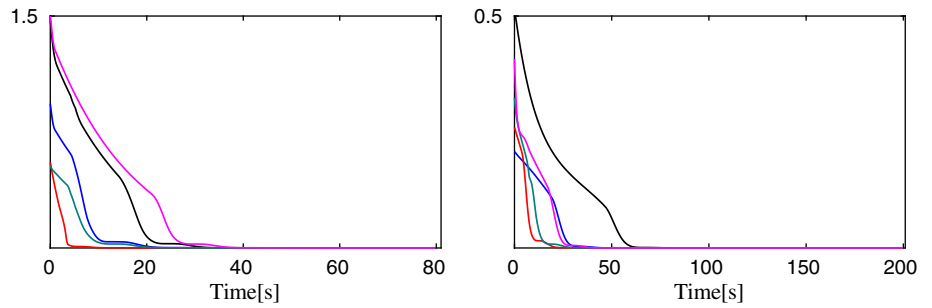
(A) Coordination performance: evolution of the coordination states (path parameters) $\gamma^{[i]}$
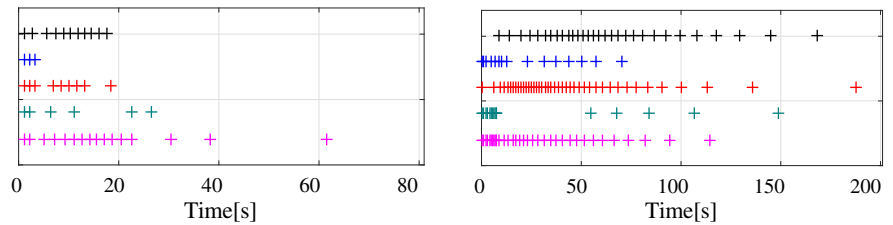
(B) Broadcast time instants

FIGURE 9 Performance of
coordination and communications. Left
(triangular formation), right (circular
formation) [Colour figure can be viewed
at wileyonlinelibrary.com]

(C) Estimation errors $\tilde{\gamma}^{[i]}$. Solid orange is *threshold triggering functions* $\eta^{[i]}$

7 | CONCLUSIONS

We proposed a solution to the constrained CPF problem that exploits the tools of MPC, network theory, and ETCs. The main contribution of this work lies in the fact the proposed strategy is not only capable of explicitly handling practical constraints on vehicles' inputs and on the topology of the communications network, but also saves communication bandwidth. We have shown that the path following error of all vehicles error is GAS, which is a strong result for an input-constrained system. Practically, this implies that regardless of the initial positions and orientations, the vehicles always converge to and follow their assigned paths. At the coordination level, we proposed a novel distributed control law with an ETC mechanism for the synchronization of multi agent nonlinear system that takes into account the agent input constraints. Future work will aim at implementing the proposed control method in the Medusa vehicles that are property of IST, and assess their performance at sea.[3]

CONFLICT OF INTEREST

The authors declare no potential conflict of interest.

AUTHOR CONTRIBUTIONS

A.M.P. suggested the problem of CPF with event-driven communications. N.T.H. suggested the inclusion of vehicle constraints and the use of MPC techniques, formulated the problem mathematically, and derived a solution for it. He also wrote the manuscript. A.M.P. and T.A.J. discussed with NTH the results obtained, provided positive criticism, and proposed modifications to streamline and clarify the proofs of the results. All authors edited the final version of the manuscript at length.

ORCID
Nguyen T. Hung https://orcid.org/0000-0003-2620-7336

REFERENCES
1. Klemas VV. Coastal and environmental remote sensing from unmanned aerial vehicles: an overview. *J Coast Res*. 2015;31(5):1260-1267. https://doi.org/10.2112/JCOASTRES-D-15-00005.1.
2. Kaminer I, Pascoal A, Xargay E, Hovakimyan N, Cichella V, Dobrokhodov V. *Time-Critical Cooperative Control of Autonomous Air Vehicles*. 1st ed. Prentice Hall, NJ: Butterworth-Heinemann; 2017.
3. Abreu P, Morishita H, Pascoal A, Ribeiro J, Silva H. Marine vehicles with streamers for geotechnical surveys: modeling, positioning, and control. *IFAC-PapersOnLine 2016*. 2016;49(23):458-464. https://doi.org/10.1016/j.ifacol.2016.10.448.
4. Ghabcheloo R, Aguiar AP, Pascoal A, Silvestre C, Kaminer I, Hespanha J. Coordinated path-following in the presence of communication losses and time delays. *SIAM J Control Optim*. 2009;48(1):234-265. https://doi.org/10.1137/060678993.
5. Almeida J, Silvestre C, Pascoal A. Cooperative control of multiple surface vessels with discrete-time periodic communications. *Int J Robust Nonlin Control*. 2012;22(4):398-419. https://doi.org/10.1002/rnc.1698.
6. Olfati-Saber R, Fax JA, Murray RM. Consensus and cooperation in networked multi-agent systems. *Proc IEEE*. 2007;95(1):215-233. https://doi.org/10.1109/JPROC.2006.887293.
7. Rucco A, Aguiar AP, Fontes FA, Pereira FL, Sousa DJB. *A model predictive control-based architecture for cooperative path-following of multiple unmanned aerial vehicles*. Cham: Springer. 2015. 141–160.
8. Alessandretti A, Aguiar AP. A distributed model predictive control scheme for coordinated output regulation. Paper presented at: Proceedings of the 20th IFAC World Congress IFAC-PapersOnLine 2017; 50(1):8692-8697. https://doi.org/10.1016/j.ifacol.2017.08.1550.
9. Aguiar AP, Pascoal AM. Coordinated path-following control for nonlinear systems with logic-based communication. Paper presented at: Proceedings of the 46th Decision and Control; 2007:1473-1479; IEEE.

10. Rego FC, Hung NT, Jones CN, Pascoal AM, Aguiar AP. Cooperative path-following control with logic-based communications: theory and practice. *Navigation and Control of Autonomous Marine Vehicles*. Michael Faraday House, Stevenage: IET; 2019:187-224.

11. Xu Y, Hespanha JP. Optimal communication logics in networked control systems. Paper presented at: Proceedings of the 43rd IEEE Conference on Decision and Control; 2004:3527-3532.

12. Jain RP, Aguiar AP. Sousa DJB. cooperative path following of robotic vehicles using an event-based control and communication strategy. *IEEE RobotAutom Lett*. 2018;3(3):1941-1948. https://doi.org/10.1109/LRA.2018.2808363.

13. Fan Y, Liu L, Feng G, Wang Y. Self-triggered consensus for multi-agent systems with zeno-free triggers. *IEEE Trans Autom Control*. 2015;60(10):2779-2784. https://doi.org/10.1109/TAC.2015.2405294.

14. Cichella V, Kaminer I, Dobrokhodov V, et al. Cooperative path following of multiple multirotors over time-varying networks. *IEEE Trans Autom Sci Eng*. 2015;12(3):945-957. https://doi.org/10.1109/TASE.2015.2406758.

15. Cao KC, Jiang B, Yue D. Cooperative path following control of multiple nonholonomic mobile robots. *ISA Trans*. 2017;71:161-169. https://doi.org/10.1016/j.isatra.2017.06.028.

16. Klausen K, Fossen TI, Johansen TA, Aguiar AP. Cooperative path-following for multirotor UAVs with a suspended payload. Paper presented at: Proceedings of 2015 IEEE Conference on Control Applications (CCA); 2015:1354-1360; IEEE.

17. Lapierre L, Soetanto D, Pascoal A. Nonsingular path following control of a unicycle in the presence of parametric modelling uncertainties. *Int J Robust Nonlin Control*. 2006;16(10):485-503. https://doi.org/10.1002/rnc.1075.

18. Abreu PC, Botelho J, Góis P, et al. The MEDUSA class of autonomous marine vehicles and their role in EU projects. *OCEANS 2016*. Piscataway, NJ: IEEE; 2016:1-10.

19. Bibuli M, Bruzzone G, Caccia M, Lapierre L. Path-following algorithms and experiments for an unmanned surface vehicle. *J Field Robotics*. 2009;26(8):669-688. https://doi.org/10.1002/rob.20303.

20. Hung NT, Rego F, Crasta N, Pascoal A. Input-constrained path following for autonomous marine vehicles with a global region of attraction. Paper presented at: 11th IFAC Conference on Control Applications in Marine Systems, Robotics, and Vehicles CAMS IFAC-PapersOnLine 2018; 2018;51(29):348-353. https://doi.org/10.1016/j.ifacol.2018.09.499.

21. Dunbar WB, Murray RM. Distributed receding horizon control for multi-vehicle formation stabilization. *Automatica*. 2006;42(4):549-558. https://doi.org/10.1016/j.automatica.2005.12.008.

22. Muller MA, Reble M, Allgöwer F. A general distributed MPC framework for cooperative control. 18th IFAC World CongressIFAC Proc Volumes 2011; 44(1):7987-7992. https://doi.org/10.3182/20110828-6-IT-1002.02884.

23. Hassan K. *Nonlinear Systems*. 3rd ed. Upper Saddle River,NJ: Prentice Hall; 2002.

24. Sontag ED. Input to state stability: basic concepts and results. *Nonlinear and Optimal Control Theory: Lectures Given at the C.I.M.E. Summer School Held in Cetraro*. Vol 2004. Berlin, Heidelberg: Springer; 2008:163-220.

25. Seyboth GS, Dimarogonas DV, Johansson KH. Event-based broadcasting for multi-agent average consensus. *Automatica*. 2013;49(1):245-252. https://doi.org/10.1016/j.automatica.2005.12.008.

26. Hung NT, Pascoal AM. Cooperative path following of autonomous vehicles with model predictive control and event triggered communications. Paper presented at: Proceedings of the 6th IFAC Conference on Nonlinear Model Predictive Control NMPC IFAC-PapersOnLine 2018; 2018;51(20):562-567. https://doi.org/10.1016/j.ifacol.2018.11.031.

27. Hung NT, Rego FC, Pascoal AM. Event-triggered communications for the synchronization of nonlinear multi agent systems on weight-balanced digraphs. Paper presented at: Proceedings of the 2019 18th European Control Conference (ECC); June 2019:2713-2718; IEEE.

28. Kebkal K, Kebkal O, Glushko E, et al. Underwater acoustic modems with integrated atomic clocks for one-way travel-time underwater vehicle positioning. Paper presented at: Proceedings of the 2017 Underwater Acoustics Conference and Exhibition; 2017.

29. Pena d lDM, Christofides PD. Lyapunov-based model predictive control of nonlinear systems subject to data losses. *IEEE Trans Autom Control*. 2008;53(9):2076-2089. https://doi.org/10.1109/TAC.2008.929401.

30. Yu S, Li X, Chen H, Allgöwer F. Nonlinear model predictive control for path following problems. *Int J Robust Nonlin Control*. 2015;25(8):1168-1182. https://doi.org/10.1002/rnc.3133.

31. Jiang ZP, Lefeber E, Nijmeijer H. Saturated stabilization and tracking of a nonholonomic mobile robot. *Syst Control Lett*. 2001;42(5):327-332. https://doi.org/10.1016/S0167-6911(00)00104-3.

32. Andersson JAE, Gillis J, Horn G, Rawlings JB, Diehl M. CasADi – a software framework for nonlinear optimization and optimal control. *Math Program Comput*. 2018;11:1-36. https://doi.org/10.1007/s12532-018-0139-4.

33. Horn RA, Johnson CR. *Matrix Analysis*. 2nd ed. Cambridge, MA: Cambridge University Press; 2012.

34. Loría A, Panteley E. *2 Cascaded Nonlinear Time-Varying Systems: Analysis and Design*. London, UK: Springer; 2005:23-64.

APPENDIX A. PROOFS OF LEMMAS

A.1 Proof of Lemma 1

The first relation comes from the fact that without delays the estimators for $\hat{\gamma}^{[i]}$ and $\hat{\gamma}^{[ji]}$ in (21) and (22), respectively, are always initialized at the same value. Furthermore, since $v_d(\cdot)$ is identical to both estimators, $\hat{\gamma}^{[i]}(t) = \hat{\gamma}^{[ji]}(t)$ for all t (see Figure 4 as an example). The second relation stems from the fact with the ETC mechanism $\tilde{\gamma}^{[i]}$ is always enforced to satisfy $|\tilde{\gamma}^{[i]}(t)| \leq \eta^{[i]}(t)$ and, since (i) holds for all t then (ii) holds for all t. ∎

A.2 Proof of Lemma 2

Let $\mathcal{T}_k := [t_k^{[i]}, t_k^{[ji]})$ be the time interval between the instant $t_k^{[i]}$ when agent i broadcasts a message including $(t_k^{[i]}, \gamma^{[i]}(t_k^{[i]}))$ and instant $t_k^{[ji]}$ when agent $j; j \in \mathcal{N}^{[i]}$ receives this message. It is important to note that the triggering condition for agent i is independent of the communication delays. Therefore, it is possible that agent i may end up sending new messages to agent j before the first message has been received by the latter agent. At the same time, from the point of view of agent j, this agent might also receive different messages from agent i in the interval $\mathcal{T}_k$. These scenarios are illustrated in Figure A1.

We now consider the estimation error $\gamma^{[i]} - \hat{\gamma}^{[ji]}$ in the interval $\mathcal{T}_k$. Notice that in this interval $\hat{\gamma}^{[ji]}$ may be discontinuous, because whenever agent j receives a new message from agent i, $\hat{\gamma}^{[ji]}$ will be reset according to (25b). Let $t_h^{[ji]}, t_{h+1}^{[ji]}, \dots, t_{h+H}^{[ji]} \in \mathcal{T}_k$ be a sequence of time instants at which agent $j; j \in \mathcal{N}^{[i]}$ receives messages broadcast by agent i at the corresponding times $t_h^{[i]}, t_{h+1}^{[i]}, \dots, t_{h+H}^{[i]}$. Without loss of generality, we assume that $t_k^{[i]} \leq t_h^{[ji]} \leq t_{h+1}^{[ji]} \leq \dots \leq t_{h+H}^{[ji]} \leq t_k^{[ji]}$.

We now consider the estimation error $\gamma^{[i]} - \hat{\gamma}^{[ji]}$ in each interval $\mathcal{T}_h := [t_h^{[ji]}, t_{h+1}^{[ji]}) \subseteq \mathcal{T}_k$. To this end, we define a new variable $\hat{\gamma}_h^{[ji]}$ as follows

$$\hat{\gamma}_h^{[ji]}(t) = \gamma^{[i]}(t_h^{[i]}) + \int_{t_h^{[i]}}^{t} v_d(\hat{\gamma}_h^{[ji]}(\tau)) d\tau \tag{A1}$$

From (25) and (A1), it can be observed that $\hat{\gamma}^{[ji]}(t) = \hat{\gamma}_h^{[ji]}(t)$ for all $t \in \mathcal{T}_h$. This is also illustrated in Figure A1. Therefore, in the interval $\mathcal{T}_h$, instead of examining the error between $\hat{\gamma}^{[ji]}$ and $\gamma^{[i]}$, we examine the error between $\hat{\gamma}_h^{[ji]}$ and $\gamma^{[i]}$. When $t \in \mathcal{T}_h$, from (A1) we obtain

$$\hat{\gamma}_h^{[ji]}(t) = \hat{\gamma}_h^{[ji]}(t_h^{[ji]}) + \int_{t_h^{[ji]}}^{t} v_d(\hat{\gamma}_h^{[ji]}(\tau)) d\tau$$

$$= \hat{\gamma}_h^{[ji]}(t_{h+1}^{[i]}) + \int_{t_{h+1}^{[i]}}^{t} v_d(\hat{\gamma}_h^{[ji]}(\tau)) d\tau. \tag{A2}$$

From (9), it follows that

$$\gamma^{[i]}(t) = \gamma^{[i]}(t_h^{[ji]}) + \int_{t_h^{[ji]}}^{t} \left(v_d(\gamma^{[i]}(\tau)) + v_c^{[i]}(\tau) \right) d\tau$$

$$= \gamma^{[i]}(t_{h+1}^{[i]}) + \int_{t_{h+1}^{[i]}}^{t} \left(v_d(\gamma^{[i]}(\tau)) + v_c^{[i]}(\tau) \right) d\tau. \tag{A3}$$
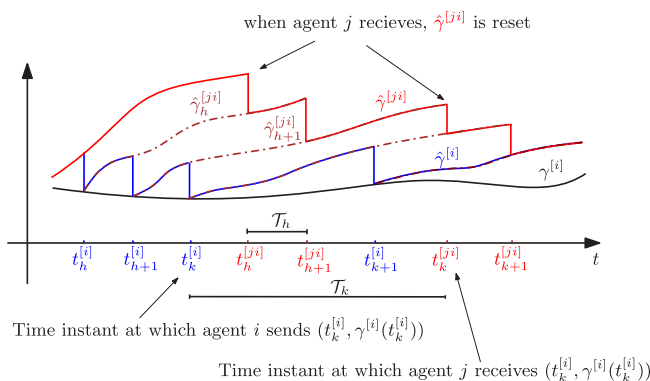

FIGURE A1 Illustration of the evolution of variables with communication delays. Solid black denotes the true trajectory of $\gamma^{[i]}$. Solid blue denotes the estimate of $\gamma^{[i]}$ at agent i. Solid red denotes the estimate of $\gamma^{[i]}$ at agent j, namely $\hat{\gamma}^{[ji]}$, while dot-brown denotes the auxiliary variable $\hat{\gamma}_h^{[ji]}$ [Colour figure can be viewed at wileyonlinelibrary.com]

Subtracting both sides of (A2) from Equation (A3) and taking absolute values, yields

$$|\gamma^{[i]}(t) - \hat{\gamma}_h^{[ji]}(t)| \leq |\gamma^{[i]}(t_{h+1}^{[i]}) - \hat{\gamma}_h^{[ji]}(t_{h+1}^{[i]})| + \underbrace{\int_{t_{h+1}^{[i]}}^t |v_d(\gamma^{[i]}(\tau)) - v_d(\hat{\gamma}_h^{[ji]}(\tau))|d\tau + \int_{t_{h+1}^{[i]}}^t |v_c^{[i]}(\tau)|d\tau}_{=:A}. \tag{A4}$$

Notice that at the time $t_{h+1}^{[i]}$ at which $\gamma^{[i]}$ is reset, $|\gamma^{[i]}(t_{h+1}^{[i]}) - \hat{\gamma}_h^{[ji]}(t_{h+1}^{[i]})| \leq \eta^{[i]}(t_{h+1}^{[i]})$ (see also Figure A1). Since $t_{h+1}^{[i]}$ for all $t \in \mathcal{T}_h$, $\eta^{[i]}(t_{h+1}^{[i]}) \leq \overline{\eta}^{[i]}(t)$. Therefore, $|\gamma^{[i]}(t_{h+1}^{[i]}) - \hat{\gamma}_h^{[ji]}(t_{h+1}^{[i]})| \leq \overline{\eta}^{[i]}(t)$. In addition, from (A4) we obtain

$$A \leq (v_{dmax} - v_{dmin} + k_{max})(t - t_{h+1}^{[i]}) = (v_{dmax} - v_{dmin} + k_{max})\Delta_{h+1}^{[ji]}(t).$$

Since $t_{h+1}^{[i]} \leq t$ for all $t \in \mathcal{T}_h$, $\Delta_{h+1}^{[ji]}(t) \leq \overline{\Delta}^{[i]}(t)$. We conclude that for all $t \in \mathcal{T}_h$

$$|\gamma^{[i]}(t) - \hat{\gamma}^{[ji]}(t)| \leq \overline{\eta}^{[i]}(t) + (v_{dmax} - v_{dmin} + k_{max})\overline{\Delta}^{[i]}(t). \tag{A5}$$

Using similar reasoning, it can be shown that in any time interval $t \in [t_{h+n}^{[ji]}, t_{h+n+1}^{[ji]}) \subseteq \mathcal{T}_k$; $n = 1, \ldots, H$, inequality (A5) also holds. Hence, we conclude that the inequality (A5) holds for all $t \geq 0$. This completes the proof. ∎

A.3 Proof of Lemma 3

The proof is done in two steps:

Feasibility. To show that the heading rate r is feasible, we compute

$$|r| = \left| -\frac{k_3 e_y u \sin e_\psi}{(1 + e_x^2 + e_y^2)e_\psi} - k_2 \tanh(e_\psi) + \kappa(\gamma)g(\gamma)v \right|$$

$$\leq 0.5 k_3 u_{max} + k_2 + \max(|\kappa(\gamma)g(\gamma)|)v_{max}.$$

Clearly, by choosing k_2, k_3 positive such that (35) is satisfied, it follows that $|r| \leq r_{max}$. Next, it is easy to check v is feasible by computing

$$|v| = \left| \frac{1}{g(\gamma)} \left(u\cos(e_\psi) + k_1 \tanh(e_x) \right) \right| \leq (|u| + k_1)/g(\gamma),$$

Notice that according to (28), $|u| \leq (v_{dmax} + k_c)\max(g(\gamma))$. Hence, Choosing k_1 such that (35) is satisfied and using condition (33), it follows that $|v| \leq v_{max}$.

Global asymptotic stability. Replacing $\mathbf{u}$ in (29) with the control law (34) yields the closed-loop path following error system described by

$$\dot{\mathbf{x}} = \mathbf{f}(\mathbf{x}, u) = \begin{bmatrix} u\cos(e_\psi)e_y + k_1\tanh(e_x)(1 - e_y) \\ u\left(\sin(e_\psi) - e_x\cos(e_\psi)\right) - k_1\tanh(e_x)e_x \\ -\frac{k_3 e_y \sin(e_\psi)}{(1+e_x^2+e_y^2)e_\psi}u - k_2\tanh(e_\psi) \end{bmatrix}, \tag{A6}$$

where u is given by (28). Notice that system (A6) is nonautonomous since $u(t)$ is in general a function of time (as v_c depends on the the triggering functions that are time-dependent). To show that $\mathbf{x} = \mathbf{0}$ is GAS we need to show that

(i) $\mathbf{x} = \mathbf{0}$ is stable and
(ii) $\mathbf{x} = \mathbf{0}$ is globally attractive, that is, $\lim_{t\to\infty} \mathbf{x}(t) = \mathbf{0}$ for any initial condition $\mathbf{x}(t_0)$.

(i). Stability.

Computing the time derivative of the Lyapunov function given in (36) along the trajectory of (A6) yields

$$\dot{V}(\mathbf{x}) = -\frac{k_3 k_1 e_x \tanh(e_x)}{1 + e_x^2 + e_y^2} - k_2 e_\psi \tanh(e_\psi) \leq 0 \tag{A7}$$

for all $\mathbf{x}$. Using the fact that $\dot{V}$ is a negative semidefinite function and V is radially unbounded, it follows that $\mathbf{x} = \mathbf{0}$ is stable and $\mathbf{x}(t)$ is bounded given any initial condition $\mathbf{x}(t_0)$ at an arbitrary initial time t_0.

(*ii*). $\mathbf{x} = \mathbf{0}$ is globally attractive.

From (A7), it can be seen that $\dot{V}$ is negative everywhere except on the line $\Omega := \{\mathbf{x}|e_x = 0, e_\psi = 0\}$ where $\dot{V}(\mathbf{x}) = 0$. For the system to maintain the $\dot{V}(\mathbf{x}) = 0$ condition, the trajectory of the system must be confined to the line Ω. Unless $e_y = 0$, this is impossible because from the third equation of (A6)

$$\dot{e}_\psi \equiv 0 \Rightarrow -\frac{k_3 e_y(t)}{1 + e_x^2(t) + e_y^2(t)} u(t) \equiv 0. \tag{A8}$$

Because $u(t) \neq 0$ for all t, (A8) holds iff $e_y(t) \equiv 0$. This implies that the system can maintain the $\dot{V}(\mathbf{x}) = 0$ condition only at the origin $\mathbf{x} = \mathbf{0}$. Therefore, $V(\mathbf{x}(t))$ must decrease toward to zero. As a consequence, $\mathbf{x} \to \mathbf{0}$ as $t \to \infty$. This completes the proof.

Regarding this proof, two interesting observations can be made. First, no matter what $u(t)$ is, as long as it does not go through zero the path following error always converges to zero. This means that the update of correction speed from the coordination layer does not affect stability of the path following error system. Hence, from a stability point of view, the path following control layer is decoupled from the coordination layer. Second, the fact that convergence of $\mathbf{x}(t)$ to zero is obtained if $u(t) > 0$ for all t is intuitive, in the sense that forward motion is required to ensure that, by rotating, the vehicle will be able to track the "virtual reference" (the origin of the parallel transport attached to the path).

Remark 12. Recall that the reference speed u assigned for the vehicle, in general, is a function of time due to the ETC mechanism; and therefore the resulting path following error system is nonautonomous. This is the reason why we did not use LaSalle's invariance principle to conclude the stability in the proof. Note that this is different from the single path following studied in[20] where the speed of the vehicle depends only on the path parameter, which makes the path following error system autonomous; and therefore the proof of stability can be done using the invariance principle.

APPENDIX B. SUPPLEMENTAL LEMMAS

The following lemmas will be used in the proof of some theorems and corollaries.

B.1 Lemma on connectivity of graph

Lemma 4. *Let L be the Laplacian matrix of a graph $\mathcal{G}$. Suppose $\mathcal{G}$ is undirected and connected. Then, for any vector $\mathbf{x} \in \mathbb{R}^N$ and $\mathbf{x} \perp 1$, the following inequalities hold:*

$$\lambda_2\|\mathbf{x}\|^2 \leq \mathbf{x}^\mathrm{T} L \mathbf{x} \leq \lambda_N\|\mathbf{x}\|^2, \tag{B1a}$$

$$\lambda_2\|\mathbf{x}\| \leq \|L\mathbf{x}\| \leq \lambda_N\|\mathbf{x}\|, \tag{B1b}$$

where λ_2 and $\lambda_N \in \mathbb{R}_{>0}$ are the second smallest and the largest eigenvalues of L, respectively.

Proof. Let $\mathbf{v}_1, \mathbf{v}_2, \ldots, \mathbf{v}_N \in \mathbb{R}^N$ be the eigenvectors of L associated with the eigenvalues $\lambda_1, \lambda_2, \ldots, \lambda_N$. Let $\lambda_1 \leq \lambda_2 \leq \ldots \leq \lambda_N$. Since the graph is undirected and connected, it is well-know that $\lambda_1 = 0$ and $\mathbf{v}_1 = \mathbf{1}$, and $\lambda_i > 0$ for all $2 \leq i \leq N$. From the Courant-Fischer theorem in Reference 33 it follows that

$$\lambda_2 = \min_{\mathbf{x} \neq \mathbf{0} \text{ and } \mathbf{x} \perp \mathbf{1}} \frac{\mathbf{x}^\mathrm{T} L \mathbf{x}}{\mathbf{x}^\mathrm{T}\mathbf{x}}, \quad \lambda_N = \max_{\mathbf{x} \neq \mathbf{0}} \frac{\mathbf{x}^\mathrm{T} L \mathbf{x}}{\mathbf{x}^\mathrm{T}\mathbf{x}}.$$

Therefore, the inequality (B1a) holds. Now we consider the matrix $B = LL$. It can be easily checked that B has an eigenvalue at 0 and with an associated eigenvector $\mathbf{1}$. Let $\lambda_i(B)$ be the eigenvalues of B, we obtain $\lambda_i(B) = \lambda_i^2, i = 1, \ldots, N$. Applying again the Courant-Fischer theorem, it follows that for any $\mathbf{x} \in \mathbb{R}^N$ and $\mathbf{x} \perp \mathbf{1}$, $\lambda_2(B)\|\mathbf{x}\|^2 = \lambda_2^2\|\mathbf{x}\|^2 \leq \mathbf{x}^\mathrm{T} B \mathbf{x} = \|L\mathbf{x}\|^2 \leq \lambda_N(B)\|\mathbf{x}\|^2 = \lambda_N^2\|\mathbf{x}\|^2$. Therefore, the inequality (B1b) holds. ∎

B.2 Lemma on tan hyperbolic function

Lemma 5. *Let* $\mathbf{y} \in \mathbb{R}^n$ *and* $\theta \in (0, 1)$. *Then, for all* $\mathbf{x} \in \mathbb{R}^n$ *such that* $\|\mathbf{x}\|_\infty \geq (2n-1)\|\mathbf{y}\|_\infty/\theta$ *the following inequality holds*

$$-\mathbf{x}^{\mathsf{T}}\mathbf{tanh}(\mathbf{x}+\mathbf{y}) \leq -\frac{\|\mathbf{x}\|_\infty}{2}\tanh\left((1-\theta)\|\mathbf{x}\|_\infty\right).$$

Proof. In the proof, we will use the following important facts:

Let $a, b \in \mathbb{R}, \alpha > 0$. If $|\alpha a| \geq |b|$ then

Fact 1: $a \tanh(\alpha a + b) \geq 0$ and

Fact 2: $a \tanh(\alpha a + b) \geq |a| \tanh(|\alpha a| - |b|)$.

Fact 1 can be checked by noting that if $|a| \geq |b|$ then a and $\tanh(a + b)$ have the same sign. *Fact 2* holds because tanh is a monotonically increasing function of its argument.

The proof of the Lemma proceeds as follows:

Let $\bar{x} := \|\mathbf{x}\|_\infty, \bar{y} := \|\mathbf{y}\|_\infty$, and $m := (2n-1)\bar{y}/\theta$ and

$$S := -\mathbf{x}^{\mathsf{T}}\mathbf{tanh}(\mathbf{x}+\mathbf{y}) = -\sum_{i=1}^{n} x_i \tanh(x_i + y_i) \tag{B2}$$

Recall from *Fact 1* that $x_i \tanh(x_i + y_i) \geq 0$ if $|x_i| \geq |y_i|$ and define the two sets

$$S_1 := \{x_i : |x_i| \geq \bar{y}\} \text{ and } S_2 := \{x_i : |x_i| < \bar{y}\}.$$

With the above definition, Equation (B2) can be rewritten as

$$S = -\underbrace{\sum_{x_i \in S_1} x_i \tanh(x_i + y_i)}_{=:C_1} - \underbrace{\sum_{x_i \in S_2} x_i \tanh(x_i + y_i)}_{=:C_2} \tag{B3}$$

Using Fact 1, we conclude that all the products in the sum of C_1 are negative. Later, we will show that C_2 is bounded. We will henceforth use the condition given in the Lemma that $\bar{x} \geq m$. Note that $m > \bar{y}$ for all $\theta \in (0, 1)$, and therefore $\bar{x} > \bar{y}$. It follows that the set S_1 has at least one element, that is, $|S_1| \geq 1$ and therefore $|S_2| \leq n - 1$. Let i^* be the index such that $x_{i^*} \in S_1$ and $|x_{i^*}| = \bar{x}$. Since $x_i \tanh(x_i + y_i) \geq 0$ for all $x_i \in S_1$, it follows that

$$\begin{aligned} C_1 &\leq -x_{i^*}\tanh(x_{i^*} + y_{i^*}) \\ &= -x_{i^*}\tanh((1-\theta)x_{i^*} + \theta x_{i^*} + y_{i^*}) \\ &= -\underbrace{\frac{x_{i^*}\tanh((1-\theta)x_{i^*})}{\sigma}}_{=:D_1} - \underbrace{\frac{x_{i^*}\tanh(\theta x_{i^*} + y_{i^*})}{\sigma}}_{=:D_2}, \end{aligned} \tag{B4}$$

where $\sigma := 1 + \tanh((1-\theta)x_{i^*})\tanh(\theta x_{i^*} + y_{i^*})$. Because $|\theta x_{i^*}| = \theta\bar{x} \geq \theta m > \bar{y} \geq y_{i^*}$, using *Fact 1* it follows that $0 \leq \tanh((1-\theta)x_{i^*})\tanh(\theta x_{i^*} + y_{i^*}) \leq 1$. Therefore, $1 \leq \sigma \leq 2$. Recall that $|x_{i^*}| = \bar{x} = \|\mathbf{x}\|_\infty$ and $1 \leq \sigma \leq 2$ we can conclude that

$$D_1 \leq -\frac{\|\mathbf{x}\|_\infty}{2}\tanh\left((1-\theta)\|\mathbf{x}\|_\infty\right). \tag{B5}$$

Furthermore, since $|\theta x_{i^*}| \geq y_{i^*}$, using *Fact 2*, it follows that

$$D_2 \leq -\frac{|x_{i^*}|\tanh(|\theta x_{i^*}| - |y_{i^*}|)}{2} \leq -\frac{(2n-1)}{2\theta}\bar{y}\tanh((2n-1)\bar{y} - \bar{y}) \leq -(n-1)\bar{y}\tanh(2(n-1)\bar{y}). \tag{B6}$$

At this point, we observe that

- For $n = 1$, $D_2 \leq 0$. Notice also that $C_2 = 0$ because $|S_2| = 0$.
- For $n \geq 2$, $D_2 \leq -(n-1)\bar{y}\tanh(2\bar{y})$. Also, since $|x_i| \leq \bar{y}$ for all $x_i \in C_2$ and $|S_2| \leq (n-1)$, it follows that $C_2 \leq (n-1)\bar{y}\tanh(2\bar{y})$.

We conclude that $D_2 + C_2 \leq 0$ for all $n \geq 1$. As consequence, $S = D_1 + D_2 + C_2 \leq D_1$. Hence, from (B5) we conclude that

$$S = -\mathbf{x}^{\mathrm{T}}\mathbf{tanh}(\mathbf{x} + \mathbf{y}) \leq -\frac{\|\mathbf{x}\|_\infty}{2}\tanh((1-\theta)\|\mathbf{x}\|_\infty)$$

for all $\theta \in (0, 1)$ and $\|\mathbf{x}\|_\infty \geq (2n-1)\|\mathbf{y}\|_\infty/\theta$. This concludes the proof. ∎

APPENDIX C. PROOFS OF THEOREMS

C.1 Proof of Theorem 1
The proof of the theorem is done in two steps.
Step 1: Feasibility. Recall that $u^{[i]} = g^{[i]}(\gamma^{[i]})(v_d(\gamma^{[i]}) + v_c^{[i]})$, Replacing $v_c^{[i]}$ by (13) yields

$$u^{[i]} = g^{[i]}(\gamma^{[i]})\left(v_d(\gamma^{[i]}) - k_c^{[i]}\tanh\left(\sum_{j\in\mathcal{N}^{[i]}} z^{[i]} - z^{[j]}\right)\right).$$

Since $g^{[i]}(\gamma^{[i]})$ and $k_c^{[i]}$ are positive for all $\gamma^{[i]}$ and $i \in \mathcal{N}$, it follows that

$$g^{[i]}(\gamma^{[i]})(v_d(\gamma^{[i]}) - k_c^{[i]}) \leq u^{[i]} \leq g^{[i]}(\gamma^{[i]})(v_d(\gamma^{[i]}) + k_c^{[i]}).$$

Furthermore, because $k_c^{[i]} \leq c_u/g_{\max}^{[i]}$ for all $i \in \mathcal{N}$ (see (14)), it follows from condition C1.2 that $u^{[i]}$ satisfies the inequality $u_{\min}^{[i]} \leq u^{[i]} \leq u_{\max}^{[i]}$ for all $i \in \mathcal{N}$, from which it can be concluded that the correction speed (13) satisfies the linear speed constraint (10).
Step 2: Global Consensus. From (11), (9) and (13) we obtain

$$\dot{z}^{[i]} = \frac{1}{v_d(\gamma^{[i]})}(v_d(\gamma^{[i]}) - k_c^{[i]}\tanh\left(\sum_{j\in\mathcal{N}^{[i]}} z^{[i]} - z^{[j]}\right)$$

$$= 1 - d^{[i]}\tanh\left(\sum_{j\in\mathcal{N}^{[i]}} z^{[i]} - z^{[j]}\right)$$

where $d^{[i]} := k_c^{[i]}/v_d(\gamma^{[i]}) > 0$ for all $\gamma^{[i]}$ and $i \in \mathcal{N}$. As a consequence, the dynamics of $\mathbf{z}$ are described by

$$\dot{\mathbf{z}} = \mathbf{1} - K\mathbf{tanh}(L\mathbf{z}), \tag{C1}$$

where $K := \mathrm{diag}(d^{[1]}, d^{[2]} \ldots, d^{[N]}) \in \mathbb{R}^{N\times N}$. We now consider the Lyapunov function candidate for the closed loop coordination system, defined as

$$V_c(\xi) = \frac{1}{2}\xi^{\mathrm{T}}L\xi. \tag{C2}$$

Intuitively, V_c measures the disagreement between the agents' states (path parameters). Notice that by the definition in (12), $\xi \perp \mathbf{1}$. Using Lemma 4 we obtain $V_c(\xi) \geq \lambda_2\|\xi\|^2/2 \geq 0$ for all ξ and $V_c(\xi) = 0$ iff $\xi = \mathbf{0}$. Therefore, V_c is a positive definite function. Computing the time derivative of V_c and using (C1), we obtain

$$\dot{V}_c = \xi L\dot{\xi} = \mathbf{z}^{\mathrm{T}}L\dot{\mathbf{z}}$$

$$= -\mathbf{z}^{\mathrm{T}}LK\mathbf{tanh}(L\mathbf{z}) = -\mathbf{q}^{\mathrm{T}}K\mathbf{tanh}(\mathbf{q}) \leq 0 \tag{C3}$$

for all ξ, where $\mathbf{q} := L\mathbf{z} = L\xi$. Because $K > 0$, $\dot{V}_c = 0$ iff $\mathbf{q} = \mathbf{0}$. Furthermore, $L\mathbf{1} = \mathbf{0}$, this implies $\dot{V}_c = 0$ when either $\xi = \mathbf{0}$ or ξ spans $\mathbf{1}$. However, by the definition in (12) ξ is always orthogonal to $\mathbf{1}$, hence $\dot{V}_c = 0$ iff $\xi = \mathbf{0}$. This implies that V_c stops decreasing if and only if $\xi = \mathbf{0}$. Therefore, we conclude that $\xi = \mathbf{0}$ is GAS. This implies that $z^{[i]}(t) = z^{[j]}(t)$ or, equivalently, $\gamma^{[i]}(t) = \gamma^{[j]}(t)$ for all $i, j \in \mathcal{N}$ as $t \to \infty$. ∎

C.2 Proof of Theorem 2

The proof is done in three steps:

Step 1: From Lemma 1, and (20) we conclude that $|e^{[i]}(t)| \leq \eta^{[i]}(t)/v_{\mathrm{dmin}}$ for all t and all $i \in \mathcal{N}$. Letting $\mathbf{e} = [e^{[1]}, e^{[2]}, \ldots, e^{[N]}]^{\mathrm{T}}$, it follows that

$$\|\mathbf{e}\|_\infty \leq \|\boldsymbol{\eta}\|_\infty / v_{\mathrm{dmin}} \leq \sqrt{N} \|\boldsymbol{\eta}\| / v_{\mathrm{dmin}}. \tag{C4}$$

Step 2: We show that the closed-loop coordination system is ISS respect to the state ξ and input $\boldsymbol{\eta}$. With the control law (18), the dynamics of $\mathbf{z}$ can be rewritten as

$$\dot{\mathbf{z}} = \mathbf{1} - K\mathbf{tanh}(L\mathbf{z} + A\mathbf{e}), \tag{C5}$$

where A is the adjacency matrix of the graph. Notice that compared with (C1), for the case continuous communications, the term $A\mathbf{e}$ can be viewed as an external disturbance. It follows from the above that the derivative of Lyapunov function candidate V_c in (C4) is given by

$$\dot{V}_c = -\mathbf{z}^{\mathrm{T}} L K \mathbf{tanh}(L\mathbf{z} + A\mathbf{e})$$
$$\leq -d_{\min} \mathbf{q}^{\mathrm{T}} \mathbf{tanh}(\mathbf{q} + A\mathbf{e}),$$

where $d_{\min} := \min_{i \in \mathcal{N}} d^{[i]} = k_{\min}/v_{\mathrm{dmax}}$ and $k_{\min} := \min_{i \in \mathcal{N}} k_{\mathrm{c}}^{[i]}$. Now, using Lemma 5 (in Appendix A), for any $\theta \in (0, 1)$ it follows that

$$\dot{V}_c \leq -d_{\min} \frac{\|\mathbf{q}\|_\infty}{2} \tanh\left((1 - \theta)\|\mathbf{q}\|_\infty\right)$$

for all $\|\mathbf{q}\|_\infty \geq (2N - 1)\|A\mathbf{e}\|_\infty/\theta$. Recall that $\mathbf{q} = L\xi$. Using Lemma 4, we obtain $\|\mathbf{q}\|_\infty = \|L\xi\|_\infty \geq \lambda_2 \|\xi\|/\sqrt{N}$. Furthermore, from (C4), it follows that $\|A\mathbf{e}\|_\infty \leq \|A\|_\infty \|\mathbf{e}\|_\infty \leq \|A\|_\infty \sqrt{N} \|\boldsymbol{\eta}\|/v_{\mathrm{dmin}}$. As a consequence,

$$\dot{V}_c \leq -d_{\min} \frac{\lambda_2 \|\xi\|}{2\sqrt{N}} \tanh\left(\frac{(1 - \theta)\lambda_2 \|\xi\|}{\sqrt{N}}\right) =: -W_1(\xi) \tag{C6}$$

for all $\|\xi\| \geq \frac{N(2N-1)\|A\|_\infty}{\lambda_2 \theta v_{\mathrm{dmin}}} \|\boldsymbol{\eta}\| =: \rho(\|\boldsymbol{\eta}\|)$.

It can bee seen that W_1 is positive definite and ρ is a class $\mathcal{K}$ function. Furthermore, V_c is bounded according to

$$\alpha_1(\|\xi\|) \leq V_c \leq \alpha_2(\|\xi\|), \tag{C7}$$

where $\alpha_1(\|\xi\|) := \lambda_2\|\xi\|^2$ and $\alpha_2(\|\xi\|) := \lambda_N\|\xi\|^2$ are two $\mathcal{K}$ class functions. Therefore, using Theorem 4.19 in[23] we conclude that V_c is an ISS-Lyapunov function for the closed-loop coordination error system. Hence, the closed loop coordination system is ISS respect to the state ξ and the input $\boldsymbol{\eta}$. This concludes the proof. ∎

C.3 Proof of Theorem 3

The proof is similar to that of Theorem 2. Using Lemma 2 and (20), it follows that

$$|e^{[i]}(t)| \leq \left(\overline{\eta}^{[i]}(t) + (v_{\mathrm{dmax}} - v_{\mathrm{dmin}} + k_{\max})\overline{\Delta}^{[i]}(t)\right)/v_{\mathrm{dmin}}.$$

Hence, from (27),

$$\|\mathbf{e}\|_\infty \leq \|\sigma\|_\infty / v_{\mathrm{dmin}} \leq \sqrt{N} \|\sigma\| / v_{\mathrm{dmin}}. \tag{C8}$$

Proceeding similarly to Step 2 in the proof of Theorem 2, we can show that the inequality (C6) holds for all $\|\boldsymbol{\xi}\| \geq \rho(\|\boldsymbol{\sigma}\|)$. Therefore, the closed loop coordination system is ISS respect to the state $\boldsymbol{\xi}$ and the input $\boldsymbol{\sigma}$. This concludes the proof. ∎

C.4 Proof of Theorem 4

Recursive Feasibility. Clearly, $\mathbf{u}_n(\mathbf{x}^{[i]}(t))$ is one of the feasible solutions of $\overline{\mathbf{u}}^{[i]}(\tau), \tau \in [t, t + \delta]$ satisfying the constraints (31g) and (31h), while the remaining $\overline{\mathbf{u}}^{[i]}(\tau), \tau \in [t + \delta, t + T_p]$ can be chosen freely in the input space $\mathbb{U}_{pf}^{[i]}$.

Stability. The proof of globally asymptotic stability relies on the contractive constraint (31h) which, together with Assumption 2, implies that

$$\dot{V}(t) = \frac{\partial V}{\partial \mathbf{x}^{[i]}} \mathbf{f}(\mathbf{x}^{[i]}(t), \mathbf{u}_{mpc}^{[i]}(t)) \leq \frac{\partial V}{\partial \mathbf{x}^{[i]}} \mathbf{f}(\mathbf{x}^{[i]}(t), \mathbf{u}_n(\mathbf{x}^{[i]}(t))) \leq 0.$$

We consider two possible cases for $\mathbf{u}_{mpc}^{[i]}(t)$. In the first case, the MPC scheme finds $\mathbf{u}_{mpc}^{[i]}(t) \neq \mathbf{u}_n(\mathbf{x}^{[i]}(t))$, yielding $\dot{V}(t) = \frac{\partial V}{\partial \mathbf{x}^{[i]}} \mathbf{f}(\mathbf{x}^{[i]}(t), \mathbf{u}_{mpc}^{[i]}(t)) < \frac{\partial V}{\partial \mathbf{x}^{[i]}} \mathbf{f}(\mathbf{x}^{[i]}(t), \mathbf{u}_n(\mathbf{x}^{[i]}(t))) \leq 0$, that is, V strictly decreasing. In the second case, $\mathbf{u}_{mpc}^{[i]}(t) = \mathbf{u}_n(\overline{\mathbf{x}}^{[i]}(t))$. Since $\mathbf{u}_n(\mathbf{x}^{[i]})$ globally stabilizes (29), we can conclude that $\mathbf{x}^{[i]} \to \mathbf{0}$ as $t \to \infty$. Thus, $\mathbf{u}_{mpc}^{[i]}(t)$ globally stabilizes (29). ∎

C.5 Proof of Theorem 5

The proof follows the results stated in Theorems 3 and 4. As stated in Theorem 4, the convergence of the path following error of each vehicle to zero is independent of the correction speed computed by the coordination layer. Without loss of generality, the dynamics of $\mathbf{x}_{pf}$ can be written as

$$\dot{\mathbf{x}}_{pf} = \mathbf{f}_{pf}(\mathbf{x}_{pf}, t). \tag{C9}$$

From Theorem 4, $\mathbf{x}_{pf} = \mathbf{0}$ is GAS. We now consider the coordination error vector $\boldsymbol{\xi}$ for the overall closed-loop CPF system. In Section 3.2, as an intermediate step in the design of a CPF control law, we assumed the vehicles were already on their assigned paths. That is, $\mathbf{x}^{[i]}$ was assumed to be zero for all $i \in \mathcal{N}$. Therefore, we did not take into account the effect of the path following layer on the coordination layer. However, in the overall closed-loop CPF system the dynamics of the path parameters in (9) can be rewritten as

$$\dot{\gamma}^{[i]} = v_d(\gamma^{[i]}) + v_c^{[i]} + d_{pf}^{[i]}, \quad i \in \mathcal{N}, \tag{C10}$$

where $d_{pf}^{[i]} : (\gamma^{[i]}, \mathbf{x}^{[i]}) \to d_{pf}^{[i]}(\gamma^{[i]}, \mathbf{x}^{[i]}); i \in \mathcal{N}$ can be viewed as an external disturbance introduced by the path following system. Notice that $d_{pf}^{[i]}$ is bounded for all $i \in \mathcal{N}$ because $v_d(\cdot), v_c^{[i]}$ are bounded and $\dot{\gamma}^{[i]} = v^{[i]}$, where $v^{[i]}$ is always bounded in the set $\mathbb{U}_{pf}^{[i]}$ for all $i \in \mathcal{N}$. In addition, it follows from Theorem 4 that $\mathbf{x}^{[i]} \to \mathbf{0}$ as $t \to \infty$ for all $i \in \mathcal{N}$. This, together with the first equation of (29) imply that as $t \to \infty$, $\dot{\gamma}^{[i]} \to v_d + v_c^{[i]}$ for all $i \in \mathcal{N}$. From (C10), this means that $d_{pf}^{[i]} \to 0$ as $t \to \infty$. With the disturbance from the path following layer, the dynamics of $\mathbf{z}$ in (C5) are rewritten as

$$\dot{\mathbf{z}} = \mathbf{1} - K\mathbf{tanh}(L\mathbf{z} + \boldsymbol{\sigma}) + \mathbf{d}_{pf}, \tag{C11}$$

where $\mathbf{d}_{pf} = [d_{bf}^{[1]}/v_d(\gamma^{[1]}), \dots, d_{bf}^{[N]}/v_d(\gamma^{[N]})]^T \in \mathbb{R}^N$. As a consequence,

$$\dot{\boldsymbol{\xi}} = W\dot{\mathbf{z}} = -WK\mathbf{tanh}(L\boldsymbol{\xi} + \boldsymbol{\sigma}) + W\mathbf{d}_{pf} =: \mathbf{f}_c(\boldsymbol{\xi}, \mathbf{x}_{pf}). \tag{C12}$$

Since $d_{pf}^{[i]} \to 0$ as $t \to \infty$, $\mathbf{d}_{pf} \to \mathbf{0}$ as $t \to \infty$. Further, $\mathbf{d}_{pf}$ is always bounded, hence the solution for $\boldsymbol{\xi}$ in (C12) is always bounded. As a consequence, from[34] we conclude that the cascaded system composed by (C9) and (C12) is ISS respect to state $\boldsymbol{\xi}_{cl} := [\mathbf{x}_{pf}^T, \boldsymbol{\xi}^T]$ and the input $\boldsymbol{\sigma}$. This completes the proof. ∎